The Plant Cell, Vol. 28: 521–536, February 2016, www.plantcell.org

The Opposing Actions of Arabidopsis CHROMOSOME TRANSMISSION FIDELITY7 and WINGS APART-LIKE1 and 2 Differ in Mitotic and Meiotic Cells

Kuntal De,[a] Pablo Bolaños-Villegas,[b,c,d] Sayantan Mitra,[a] Xiaohui Yang,[a] Garret Homan,[a] Guang-Yuh Jauh,[c,d] and Christopher A. Makaroff[a,1]

[a] Department of Chemistry and Biochemistry, Miami University, Oxford, Ohio 45056
[b] University of Costa Rica, Fabio Baudrit Agricultural Research Station, La Garita de Alajuela, 20102, Costa Rica
[c] Institute of Plant and Microbial Biology, Academia Sinica, Nankang, Taipei 11529, Taiwan
[d] Biotechnology Center, National Chung-Hsing University, Taichung 402, Taiwan

ORCID IDs: 0000-0001-9729-9608 (K.D.); 0000-0003-1729-0561 (P.B.-V.); 0000-0001-8830-4663 (G.H.); 0000-0003-3459-1331 (G.-Y.J.); 0000-0001-6237-1868 (C.A.M.)

Sister chromatid cohesion, which is mediated by the cohesin complex, is essential for the proper segregation of chromosomes during mitosis and meiosis. Stable binding of cohesin with chromosomes is regulated in part by the opposing actions of CTF7 (CHROMOSOME TRANSMISSION FIDELITY7) and WAPL (WINGS APART-LIKE). In this study, we characterized the interaction between *Arabidopsis thaliana* CTF7 and WAPL by conducting a detailed analysis of *wapl1-1 wapl2 ctf7* plants. *ctf7* plants exhibit major defects in vegetative growth and development and are completely sterile. Inactivation of WAPL restores normal growth, mitosis, and some fertility to *ctf7* plants. This shows that the CTF7/WAPL cohesin system is not essential for mitosis in vegetative cells and suggests that plants may contain a second mechanism to regulate mitotic cohesin. *WAPL* inactivation restores cohesin binding and suppresses *ctf7*-associated meiotic cohesion defects, demonstrating that WAPL and CTF7 function as antagonists to regulate meiotic sister chromatid cohesion. The *ctf7* mutation only had a minor effect on *wapl*-associated defects in chromosome condensation and centromere association. These results demonstrate that WAPL has additional roles that are independent of its role in regulating chromatin-bound cohesin.

INTRODUCTION

In eukaryotic organisms, proper chromosome segregation contributes to genomic stability, while errors in this process may lead to aneuploidy and tumor progression (Schvartzman et al., 2010). Proper chromosome segregation requires that sister chromatids remain linked together from DNA replication to anaphase. Sister chromatid cohesion is maintained by the cohesin complex, which consists primarily of a heterodimer of STRUCTURAL MAINTENANCE OF CHROMOSOME1 (SMC1) and SMC3, SISTER CHROMATID COHESION3 (SCC3), and an α-kleisin protein, either SCC1 in somatic cells or REC8 in meiotic cells (Nasmyth and Haering, 2009; Yuan et al., 2011; Seitan and Merkenschlager, 2012; Dorsett and Merkenschlager, 2013). The SMC subunits, along with the α-kleisin, are believed to form a ring structure, which is stabilized by SCC3, that embraces the replicated chromosomes (Anderson et al., 2002; Haering et al., 2002).

Cohesin is recruited onto chromosomes through the action of the SCC2/SCC4 complex primarily during G1, although cohesin binding can occur during the S and G2 phases as well if there is DNA damage (Peters et al., 2008). Prior to S phase, cohesin binding to the chromosomes is dynamic and is regulated by a complex containing the Wings apart-like (Wapl) and Precocious Dissociation of Sisters 5 (Pds5) proteins, which have been termed the releasing or antiestablishment complexes (Gandhi et al., 2006; Gerlich et al., 2006; Kueng et al., 2006; Rolef Ben-Shahar et al., 2008; Rowland et al., 2009; Sutani et al., 2009; Ouyang et al., 2013). The establishment of cohesion, which occurs during S phase (Skibbens et al., 1999; Tóth et al., 1999), is facilitated by acetylation of two adjacent lysine residues on SMC3 by the Ctf7 (Chromosome Transmission Fidelity7)/Eco1 acetyltransferase (Rolef Ben-Shahar et al., 2008; Unal et al., 2008; Zhang et al., 2008; Rowland et al., 2009). This modification of the cohesin complex appears to antagonize the action of the Wapl-Pds5 complex and to stabilize the association of cohesin with the chromatin (Rolef Ben-Shahar et al., 2008; Unal et al., 2008; Zhang et al., 2008; Rowland et al., 2009). In animal cells, acetylation of SMC3 facilitates the recruitment of sororin and displacement of Wapl to help create a stable cohesin complex (Lafont et al., 2010; Nishiyama et al., 2010). A sororin ortholog has not been detected in yeast (*Saccharomyces cerevisiae*), where SMC3 acetylation appears to directly inactivate Wpl1 releasing activity, resulting in tight binding of cohesin to the chromosomes (Schmitz et al., 2007; Nishiyama et al., 2010).

Cohesin removal from the chromosomes varies among different species, but general features of the process appear to be conserved. A large portion of the cohesins are removed from the chromosome arms prior to anaphase as part of the prophase

[1] Address correspondence to makaroca@miamioh.edu.
The author responsible for distribution of materials integral to the findings presented in this article in accordance with the policy described in the Instructions for Authors (www.plantcell.org) is: Christopher A. Makaroff (makaroca@miamioh.edu).
www.plantcell.org/cgi/doi/10.1105/tpc.15.00781

pathway, while centromeric cohesin remains in place (Gandhi et al., 2006; Kueng et al., 2006). During mitotic prophase, Polo-like kinase 1 (Plk1) and Aurora B phosphorylate SCC3 and SCC1, which facilitates the Wapl-dependent opening of the cohesin ring at the junction between SMC3 and the SCC1 Winged Helix Domain (WHD) (Losada et al., 2002; Sumara et al., 2002; Giménez-Abián et al., 2004; Arumugam et al., 2006; Lénárt et al., 2007; Nasmyth, 2011). Centromeric cohesins are protected by the Shugoshin (Sgo) protein and are therefore resistant to removal (Salic et al., 2004; Kitajima et al., 2005; McGuinness et al., 2005; Watanabe, 2005). Sgo1 is recruited to centromeres by BUB1, a spindle checkpoint protein (Kitajima et al., 2005), heterochromatin protein HP1 (Yamagishi et al., 2008), and Phosphatase 2A, which protects centromeric cohesin complexes from Plk1-mediated phosphorylation and in turn blocks the action of the Pds5-Wapl complex (Tang et al., 2006).

At the metaphase-to-anaphase transition, the anaphase promoting complex/cyclosome is activated and targets Securin and Cyclin B for ubiquitylation and subsequent degradation (Uhlmann et al., 1999; Hauf et al., 2001; Musacchio and Salmon, 2007). This leads to separase activation, which cleaves SCC1 in chromatin-localized cohesin complexes, allowing the cohesin ring to open and the sister chromatids to disjoin (Uhlmann et al., 1999). Meiotic cohesin is removed in three steps: a Wapl-dependent prophase step, followed by the separase-dependent cleavage of chromosome arm-associated REC8 at anaphase I, and then centromere-associated REC8 at anaphase II (Buonomo et al., 2000; Siomos et al., 2001; Liu and Makaroff, 2006; Yang et al., 2009; De et al., 2014).

While the general mechanism of cohesin binding and release appears to be highly conserved, results from studies in yeast, plants, and animals have identified a number of interesting differences in how organisms regulate the association and stable binding of cohesin with the chromosomes. Recent studies in *Arabidopsis thaliana* have begun to shed further insights into this process and to identify still other interesting differences. The *Arabidopsis* genome contains a single *CTF7* gene, which is similar to *CTF7*/*ECO1* genes in other organisms (Jiang et al., 2010). Plants heterozygous for *ctf7* mutations show reduced seed set, with ~25% of the seed exhibiting embryo arrest at the globular stage (Jiang et al., 2010). It was originally believed that Arabidopsis *CTF7*, like that of other organisms, is an essential gene and that homozygous *ctf7* mutants are not viable. However, it was later shown that a small number of *ctf7* progeny are produced from *Ctf7*$^{+/-}$ plants. *ctf7* plants exhibit major defects in vegetative growth and development and are completely sterile (Bolaños-Villegas et al., 2013). Likewise, expression of an inducible CTF7-RNAi construct arrests plant growth and disrupts fertility (Singh et al., 2013). At this time, it is not clear why a small number of *ctf7* plants are able to develop and grow while most *ctf7* embryos arrest early in development.

The Arabidopsis genome contains two Wapl orthologs, *WAPL1* and *WAPL2*. T-DNA insertions in each individual genes have no effect on plant growth, development, or fertility (De et al., 2014). Vegetative growth of *wapl1-1 wapl2* plants is relatively normal, although somewhat slower than the wild type. However, *wapl1-1 wapl2* plants do exhibit a reduction in male and female fertility, with meiocytes exhibiting alterations in homologous chromosome pairing and spindle formation and delays in the removal of cohesin from chromosome arms, which results in "sticky chromosomes," chromosome bridges, and the missegregation of chromosomes (De et al., 2014). Alterations were also observed early in embryo development. Mitotic chromosome alterations were observed in 20% of root tip cells; however, most mitotic cells appeared normal. Finally, a preliminary genetic interaction between *WAPL* and *CTF7* was shown by crossing *wapl1-1 wapl2* plants with plants heterozygous for a T-DNA insertion in *CTF7* (De et al., 2014).

In this study, we further characterized the interaction between Arabidopsis CTF7 and WAPL by conducting a detailed analysis of *wapl1-1 wapl2 ctf7*$^{+/-}$ and *wapl1-1 wapl2 ctf7* plants. The growth of *wapl1-1 wapl2 ctf7*$^{+/-}$ plants resembles that of *wapl1-1 wapl2*, while the growth rate of *wapl1-1 wapl2 ctf7* triple mutant plants is similar to the wild type. Like *ctf7*, *wapl1-1 wapl2 ctf7* and *wapl 1-1 wapl2* plants show defects in mitotic DNA repair and aneuploidy. Fertility in *wapl1-1 wapl2 ctf7*$^{+/-}$ and *wapl1-1 wapl2 ctf7* plants is lower than that of *wapl1-1 wapl2*, but higher than *ctf7*. Finally, WAPL inactivation was found to suppress several *ctf7*-associated cohesin defects early in meiotic prophase. Therefore, CTF7 and WAPL play antagonistic roles in cohesin binding during meiosis in Arabidopsis.

RESULTS

wapl1-1 wapl2 plants grow slightly more slowly than wild-type plants but display normal development (De et al., 2014). In contrast, *ctf7* plants are dwarf and show severe developmental abnormalities (Figure 1A). *wapl1-1 wapl2 ctf7*$^{+/-}$ plants resemble *wapl1-1 wapl2*, while normal growth is observed in *wapl1-1 wapl2 ctf7* (Figure 1B).

Inactivation of *WAPL* Fails to Rescue *ctf7*-Associated Somatic Cell Defects

CTF7 inactivation results in alterations in cell cycle progression, mitotic chromosome segregation, and DNA repair (Bolaños-Villegas et al., 2013). The normal growth and development of *wapl1-1 wapl2 ctf7* plants suggested that WAPL inactivation may suppress many of the somatic cell alterations associated with *ctf7* mutations. This possibility was investigated at several levels. Ploidy levels were analyzed in leaf cells from 9-d-old seedlings using flow cytometry to gain insight into cell cycle progression (Figure 2A; Supplemental Figure 1). A large fraction of wild-type nuclei showed a 2C DNA content (43.1% ± 0.03%), with smaller numbers containing 4C (20.0% ± 0.8%), 8C (6.0% ± 0.7%), 16C (3.2% ± 0.9%), and 32C (0.2% ± 0.03%). The proportion of 2C cells was reduced to 17.9 to 29.1% with increased numbers of polyploid cells in the different mutants, with *wapl1-1 wapl2 ctf7* plants showing the smallest fraction of 2C cells (Figure 2A). The relative DNA content of cells was increased in all the mutant lines, but no obvious pattern was observed. Most notable was the broad nature of the peaks from *wapl1-1 wapl2 ctf7* cells (Supplemental Figure 1). While most cells sorted easily into identifiable ploidy subgroups in the wild type (69.6% ± 2.6%), only 42.4% ± 0.8% of *wapl1-1 wapl2 ctf7*cells could be assigned a well-defined ploidy level (Figure 2A; Supplemental Figure 1). *ctf7* and *wapl1-1 wapl2* plants displayed relatively smaller numbers of cells with intermediate DNA content.

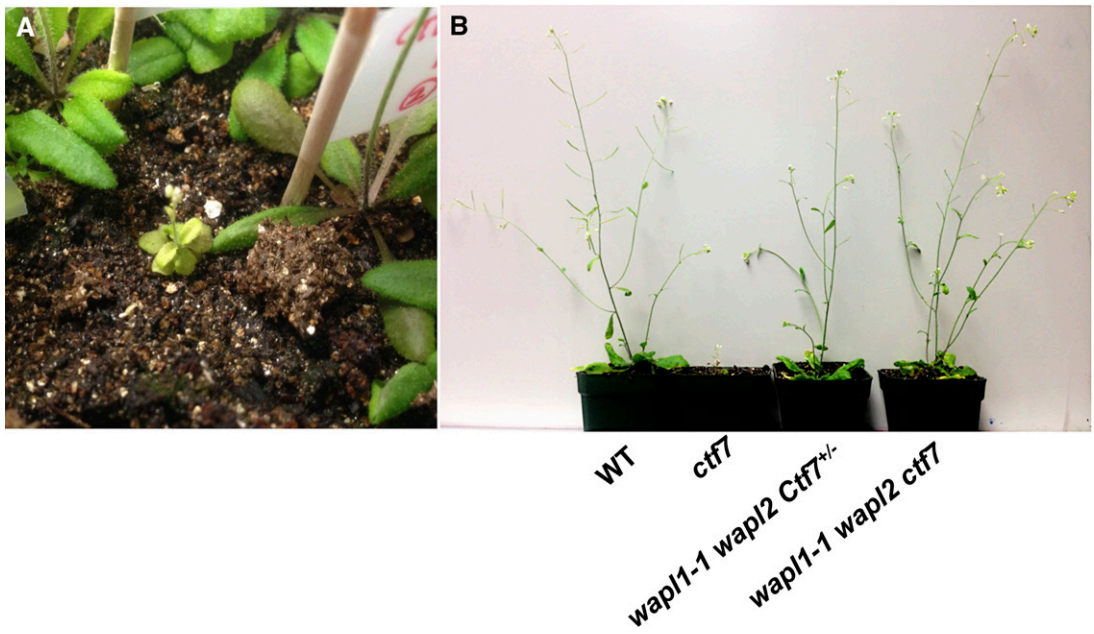

Figure 1. Inactivation of *WAPL* Rescues Growth in *ctf7* Plants.

(A) Thirty day-old *ctf7* homozygous plant.
(B) Left to right: 30-d-old wild-type, *ctf7*, *wapl1-1 wapl2 Ctf7*$^{+/-}$, and *wapl1-1 wapl2 ctf7* plants.

The apparent aneuploidy and large number of leaf cells with intermediate DNA levels suggested that mitosis may be altered in *wapl1-1 wapl2 ctf7* plants. Because the analysis of mitosis in leaf cells is technically very difficult, cell division was further analyzed by examining the roots of *wapl1-1 wapl2 ctf7* plants. No obvious defects were observed in root development or cell division patterns in the *wapl* mutants. Likewise, no obvious defects were observed in chromosome morphology, cohesin distribution, or the segregation of mitotic chromosomes in root tips of *wapl1-1 wapl2 ctf7* plants, suggesting that mitosis is normal in the mutant (Supplemental Figures 2A and 2B).

ctf7 plants are defective in DNA double-strand break (DSB) repair (Bolaños-Villegas et al., 2013). In order to determine if DNA repair efficiencies are affected in *wapl1-1 wapl2* and *wapl1-1 wapl2 ctf7* plants, we used a Trevigen Comet Assay to monitor DNA DSB levels either immediately after exposure to the cross-linking agent Mitomycin C or after a 60-min recovery period. The amount of DNA that migrated as a tail (tail-DNA) immediately after Mitomycin C treatment was relatively similar in the wild type (64% ± 7%), *ctf7* (74% ± 9%), *wapl1-1 wapl2* (67% ± 8%), and *wapl1-1 wapl2 ctf7* (68% ± 10%) plants (Supplemental Figure 3). After a 60-min recovery period, 33% ± 11% of wild-type DNA still localized within the tail, while tail DNA levels were considerably higher in *ctf7* (61% ± 9%), *wapl1-1 wapl2 ctf7* (59% ± 8%), and *wapl1-1 wapl2* (56% ± 7%) plants (Figures 2B and 2C). Calculation of DNA repair efficiencies (Kozak et al., 2009) indicated that 20% ± 9% of DSB's remained unrepaired after a 60-min recovery period in wild-type plants, while 75% ± 9%, 76% ± 8%, and 80% ± 9% of DBS's remained unrepaired in *ctf7*, *wapl1-1 wapl2*, and *wapl1-1 wapl2 ctf7* plants, respectively. Plants lacking PDS5 also show alterations in DNA repair (Pradillo et al., 2015), indicating that alterations in sister chromatid cohesion in general affect DNA repair rates.

Chromatin condensation alterations have also been identified in Arabidopsis *ctf7* mutants (Bolaños-Villegas et al., 2013). Therefore, we investigated whether leaf nuclei of *ctf7*, *wapl1-1 wapl2*, and *wapl1-1 wapl2 ctf7* plants display alterations in the level of dimethylation of histone 3 at Lys 9 ($H_3K_9me_2$), which has been correlated with condensation of chromatin at centromeres and heterochromatin in general (Kanellopoulou et al., 2005; Moissiard et al., 2012). The 4′,6-diamidino-2-phenylindole (DAPI) and $H_3K_9me_2$ signals colocalized in condensed foci in 89% ± 3% of wild-type nuclei (Figures 2D and 2E). In contrast, 15% ± 3% of the nuclei in *ctf7* leaves showed condensed signals, with most of the nuclei containing either decondensed (56% ± 8%) or severely decondensed (29% ± 6%) nuclei signals. Chromocenter decondensation was more pronounced in *wapl-1 wapl2* plants; 16% ± 4% of the nuclei showed condensed chromocenters, while 77% ± 5% and 7% ± 1% showed decondensed and severely decondensed heterochromatin, respectively. Severe heterochromatin decondensation was also observed in *wapl1-1 wapl2 ctf7* plants, with 94.3% ± 3% of nuclei showing decondensed or severely decondensed heterochromatin. Therefore, although vegetative growth is normal in *wapl1-1 wapl2 ctf7* plants, the somatic cell defects previously identified in *ctf7* plants are still present and often worse in the leaf cells of triple mutant plants.

Alterations in cell cycle progression, mitotic chromosome segregation, and DNA repair in *ctf7* plants are accompanied by elevated transcript levels for genes involved in these processes (Bolaños-Villegas et al., 2013). The presence of somatic cell alterations, coupled with the normal appearance of mitotic figures in

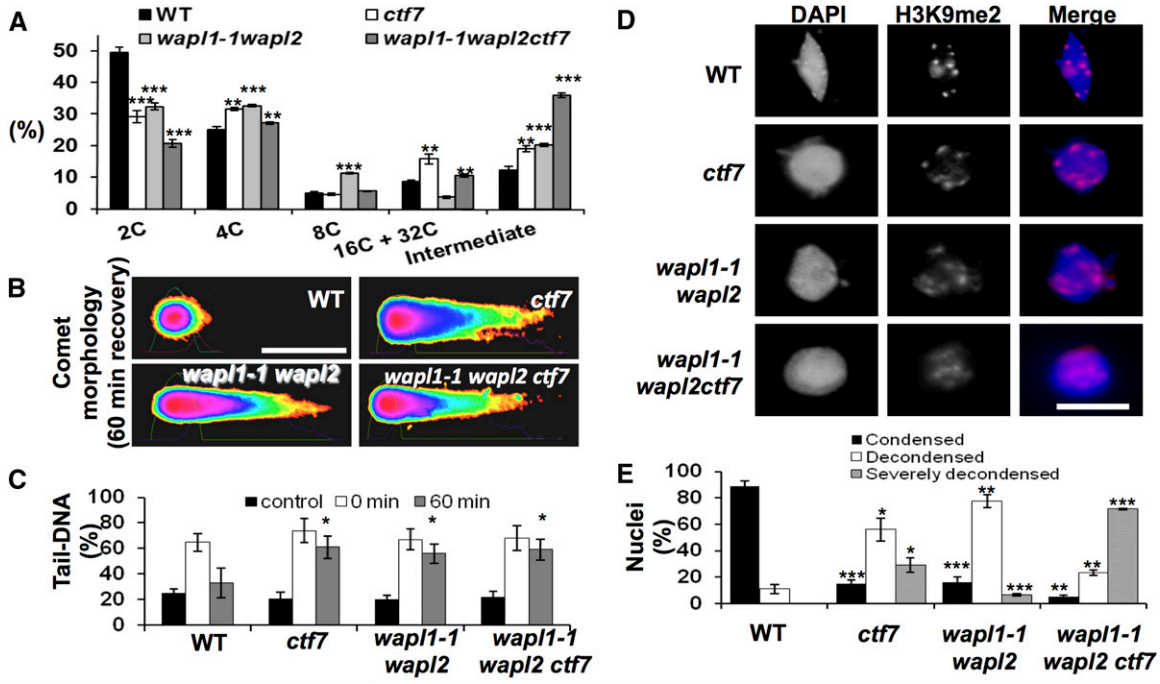

Figure 2. *wapl1-1 wapl2 ctf7* Plants Show Alterations in Cell Cycle Progression, Mitotic Chromosome Segregation, and DNA Repair.

(A) Flow cytometry data on somatic cells from 9-d-old seedlings from wild-type, *ctf7*, *wapl1-1 wapl2 ctf7*, and *wapl1-1 wapl2* plants. The percentage of cells with 2C, 4C, 8C, 16C, and "intermediate" DNA contents are shown. Data are shown as means ± SD (n = 10,000) from at least three biological samples and three technical replicates. Asterisks represent significant differences (*P < 0.5, **P < 0.01, and ***P < 0.001; Student's t test) relative to the wild type.
(B) Comet images of leaf nuclei from 9-d-old seedlings exposed to Mitomycin C analyzed before and after a 60-min recovery period. Purple and red areas correspond to areas of high DNA density, while blue, green, and yellow correspond to lower density tail-DNA. Bar = 10 μm.
(C) Percentage of tail-DNA in cells before and immediately after treatment (0 min) and after a 60-min recovery. Asterisks represent significant differences (*P < 0.5; Student's t test) relative to the wild type.
(D) Representative images of leaf nuclei from 9-d-old wild-type, *ctf7*, *wapl1-1 wapl2*, and *wapl1-1 wapl2 ctf7* plants stained for DNA with DAPI (left column) or anti-$H_3K_9me_2$ antibody (middle). Merged images are shown in the right column.
(E) Relative levels of chromocenter condensation. Sharp, well-defined anti- $H_3K_9me_2$ labeling patterns were classified as condensed chromocenters. Decondensed chromocenters appeared hazy and less well defined. Severely decondensed chromocenters were loosely shaped and hazy in appearance. Data are shown as means ± SD (n = 100) from at least three biological samples and three technical replicates. Asterisks represent significant differences (*P < 0.5, **P < 0.01, and ***P < 0.001; Student's t test) relative to the wild type. Bar = 10 μm.

the roots of *wapl1-1 wapl2 ctf7* plants raised the question of whether leaves and roots respond differently to the absence of CTF7 and/or WAPL. Therefore, we analyzed relative transcript levels for genes involved in the cell cycle and DNA repair, including kinase genes *ATM* and *ATR*, *BRCA1* (*BREAST CANCER SUSCEPTIBILITY1*), *BRCA2B*, recombinase gene *DMC1*, *CDC45* (*CELL DIVISION CYCLE45*), *CYCLINB1.1*, *SMC1*, *SMC3*, *RAD51*, and *TOPOII-α* (*TOPOISOMERASEII-α*) in different tissues. Only minor variations in transcript levels were observed for most genes in root and inflorescence samples between wild-type, *wapl1-1 wapl2*, and *wapl1-1 wapl2 ctf7* plants (Supplemental Figure 4). However, transcript levels for many of the genes were elevated (2- and 5-fold) in 1-week-old shoots of *wapl1-1 wapl2 ctf7* plants. In contrast, transcript levels were relatively normal in the shoots of *wapl1-1 wapl2* plants. Perhaps most interesting was the observation that transcript levels for the DNA repair and cell cycle control genes were elevated between 2.5- and 6-fold relative to the wild type in 1-week-old leaves of *wapl1-1 wapl2 ctf7* plants but were relatively normal in the leaves of 2-week-old plants (Figures 3A and 3B). No major differences were observed between the leaves of 1- and 2-week-old *wapl1-1 wapl2* plants.

Inactivation of *WAPL* Restores Partial Fertility to *ctf7* Plants

ctf7 plants exhibit complete sterility, while *wapl1-1 wapl2 ctf7*$^{+/-}$ and *wapl1-1 wapl2 ctf7* plants produce ~10 to 20 seeds/silique. Crossing experiments showed that both male and female fertility is affected in *wapl1-1 wapl2 ctf7*$^{+/-}$ and *wapl1-1 wapl2 ctf7* plants. In order to better understand the combined effect(s) of WAPL and CTF7 inactivation on reproduction, we analyzed pollen and female gametophyte development in the mutants. *wapl1-1 wapl2 ctf7*$^{+/-}$ plants produce on average 234 ± 18.2 pollen grains/anther (n = 20), with 41% appearing nonviable with Alexander staining (n = 1642). This compares to 229 ± 21.3 pollen grains/anther (n = 20) in *wapl1-1 wapl2* plants, with 28% of the pollen grains (n = 2752) produced appearing nonviable. Inactivation of *CTF7* in a *wapl1-1 wapl2* background reduces male fertility further, with *wapl1-1 wapl2 ctf7* plants producing 47 ± 15.5 viable pollen grains/anther

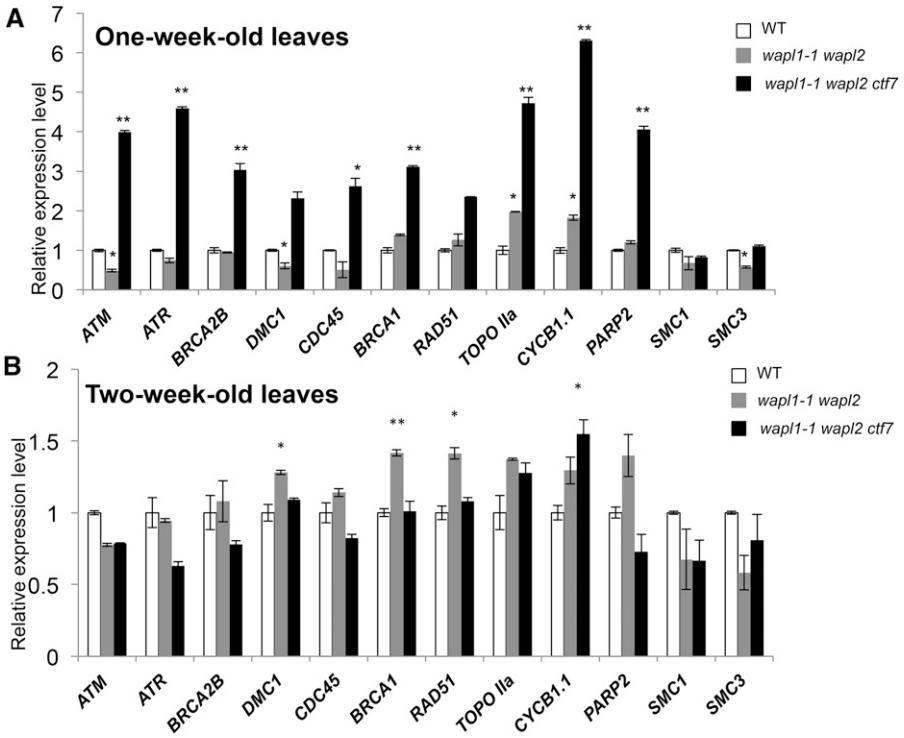

Figure 3. *wapl1-1 wapl2 ctf7* and *wapl1-1 wapl2* Exhibit Developmental Differences in DNA Repair Gene Transcript Levels.

(A) One-week-old leaves.

(B) Two-week-old leaves.

Transcript levels of ATM, ATR, BRCA2B, DMC1, CDC45, BRCA1, RAD51, TOPOII-α, CYCLINB1.1, and PARP2 were measured in Arabidopsis leaves using RT-qPCR. Graphs show representative data from two independent experiments each performed in triplicate. Error bars show the SD. Asterisks represent significant differences (*P < 0.05 and **P < 0.005; Student's *t* test) relative to the wild type.

(*n* = 16). Wild-type plants produce 458 ± 23.8 pollen grains/anther (*n* = 10), essentially all of which is viable. *wapl1-1 wapl2 ctf7* plants produce a large number of altered tetrads, with <5% of the "tetrads" examined (*n* = 512) appearing normal (Figure 4A). A mixture of polyads (31%), dyads (15%), triads (8%), and abnormal tetrads (24%) were observed (Figure 4B). A relatively high frequency of "tetrads" containing partially fused microspores were also observed, suggesting that there may also be defects in cytokinesis. In contrast, wild-type anthers contained 100% normal tetrads (*n* = 300).

Approximately 28% of *wapl1-1 wapl2* ovules (*n* = 1689) abort prior to fertilization, with 23% of the seed (*n* = 2022) produced appearing shrunken and shriveled. In contrast, ~40% of *wapl1-1 wapl2 ctf7*$^{+/-}$ ovules abort prior to fertilization, with ~50% of the fertilized ovules producing shrunken and shriveled seed (*n* = 2036). In *wapl1-1 wapl2 ctf7* plants, an average of 53.9% of the ovules/silique (*n* = 30) abort prior to fertilization and 8.1% of the seed produced (*n* = 370) is shrunken/shriveled. Analysis of ovule development identified developmental defects early in female gametophyte development in *wapl1-1 wapl2 ctf7* plants, with ovules arresting at several different developmental stages. Approximately 34% of the ovules arrested at FG0, with no identifiable nuclei (Figure 4C, i); another 12% of the ovules arrested at FG1 with one nucleus (Figure 4C, ii). Smaller numbers of ovules arrested at FG2 (4%) with two nuclei (Figure 4C, iii), and at later stages of development, including FG3-FG6 (8.6%). Ultimately, ~40% of the ovules observed (*n* = 392) matured to FG7 (Figure 4C, iv).

The siliques of *wapl1-1 wapl2 ctf7* plants contained ~8% shrunken/shriveled seed, suggesting there are also defects in embryo and/or endosperm development. An examination of cleared seeds in siliques of self-fertilized *wapl1-1 wapl2 ctf7* plants showed that ~7% of the seed contained abnormal embryos (*n* = 20 siliques). Alterations in the suspensor were observed early in development in ~2% of the seeds examined (*n* = 50; Figure 4D, i). Defects in embryo development were observed as early as the two cell stage when instead of the typical vertical division of the apical cell, 3% of the mutant embryos performed a horizontal division (Figure 4D, iv). Another common defect, which was observed in 2% of the fertilized seed, involved either abnormal or uncontrolled division during the late globular stage (Figure 4D, v). Approximately 23% of *wapl1-1 wapl2* developing seeds exhibit embryo defects (De et al., 2014) compared with the 7% observed in *wapl1-1 wapl2 ctf7* plants, suggesting that inactivation of CTF7 partially rescues embryo defects associated with *wapl1-1 wapl2* plants.

Inactivation of *WAPL* Suppresses *ctf7*-Associated Meiotic Defects

The observation that anthers of *wapl1-1 wapl2 ctf7* plants contain abnormal tetrads along with the presence of ovules that arrest at

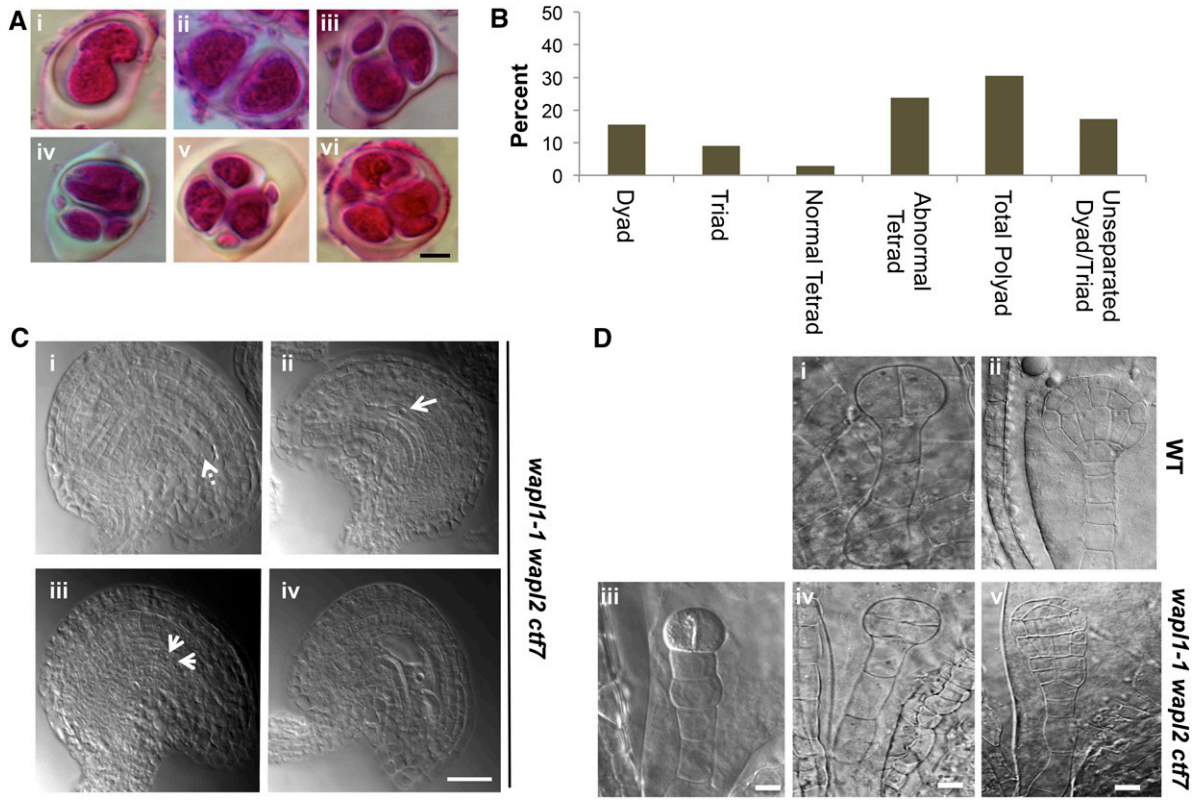

Figure 4. Pollen, Ovule, and Embryo Development Is Defective in *wapl1-1 wapl2 ctf7* Plants.

(A) Alexander staining showing alterations in tetrad formation in *wapl1-1 wapl2 ctf7*, monad (i), dyad (ii), triad (iii), abnormal tetrad (iv), polyads with five (v), and seven uneven (vi) microspores. Bar = 5 μm.

(B) Relative distribution of different types of polyads in *wapl1-1 wapl2 ctf7* plants.

(C) Female gametophytes of the triple mutant *wapl1-1 wapl2 ctf7* often abort early during development. Cleared ovules from stages FG0, FG1, FG2, and FG7 in *wapl-1 wapl2 ctf7* are shown. (i) Ovule arrested at FG0, with no identifiable nuclei. (ii) FG1 arrested ovule with one nucleus. (iii) FG2 arrested ovule with two nuclei. (iv) Normal appearing ovule at FG7. Solid arrows indicate nuclei, while the dashed arrow denotes no trace of a nucleus. Bar = 5 μm.

(D) Embryonic patterning is defective in *wapl1-1 wap2 ctf7* fertilized ovules. Fertilized ovules of wild type (i and ii) and *wapl1-1 wapl2 ctf7* (iii to v) plants were cleared in Hoyer's solution and viewed using differential interference contrast microscopy. Bars = 10 μm.

FG1 suggested that meiotic defects are likely present in the plants. Therefore, meiosis was investigated in male meiocytes of *wapl1-1 wapl2 ctf7* plants and compared with *wapl1-1 wapl2* and *ctf7* plants.

In contrast to the wild type (Figures 5A to 5D and 5Q to 5T), *ctf7* plants exhibit defects in chromosome cohesion and condensation beginning in leptotene, followed by a failure of homologous chromosomes to align and pair properly during zygotene and pachytene (Bolaños-Villegas et al., 2013) (Figures 5E to 5G). A mixture of uncondensed chromatin, apparent chromosome fragments, unpaired chromosomes, and possibly some bivalents is typically observed at diakinesis (Figure 5F) followed by a mass of DNA in metaphase I cells (Figure 5G). Chromosome bridges, uneven chromosome segregation, and lagging chromosomes are observed during anaphase I, followed by randomly distributed chromosomes during telophase I (Figure 5F). Early stages of meiosis are relatively normal in *wapl1-1 wapl2* plants; however, ~60% of cells show nonspecific association of heterochromatin regions at zygotene/pachytene (Figure 5I), followed by incomplete synapsis in a small subset (15%) of these cells (De et al., 2014). The most dramatic alterations are observed beginning at diakinesis, when chromosomes condense into large intertwined chromatin masses (Figure 5J) that continue to appear primarily as one intertwined mass at metaphase I (Figure 5K). Most cells contain stretched chromosomes that do not separate properly with chromosome bridges and lagging chromosomes observed by late anaphase I and telophase I (Figure 5L). Twenty or more chromosomes/chromosome fragments are typically observed beginning at telophase I.

Analysis of *wapl1-1 wapl2 ctf7* plants revealed that early stages of meiosis are relatively normal, with no obvious alterations in chromosome cohesion or condensation or the pairing of homologous chromosomes during leptotene, zygotene, and pachytene (Figure 5M). However, abnormalities were observed starting at diplotene, when the chromosomes typically failed to desynapse properly, with bivalents appearing as unresolved masses of DNA at diakinesis and metaphase I (Figures 5N and 5O). While similar to the situation in *wapl1-1 wapl2*, the sticky nature of the chromosomes was less severe in triple mutant plants. Homologous chromosomes failed to segregate properly during anaphase I (Figure 5P), resulting in chromosome bridges, uneven chromosome segregation, and

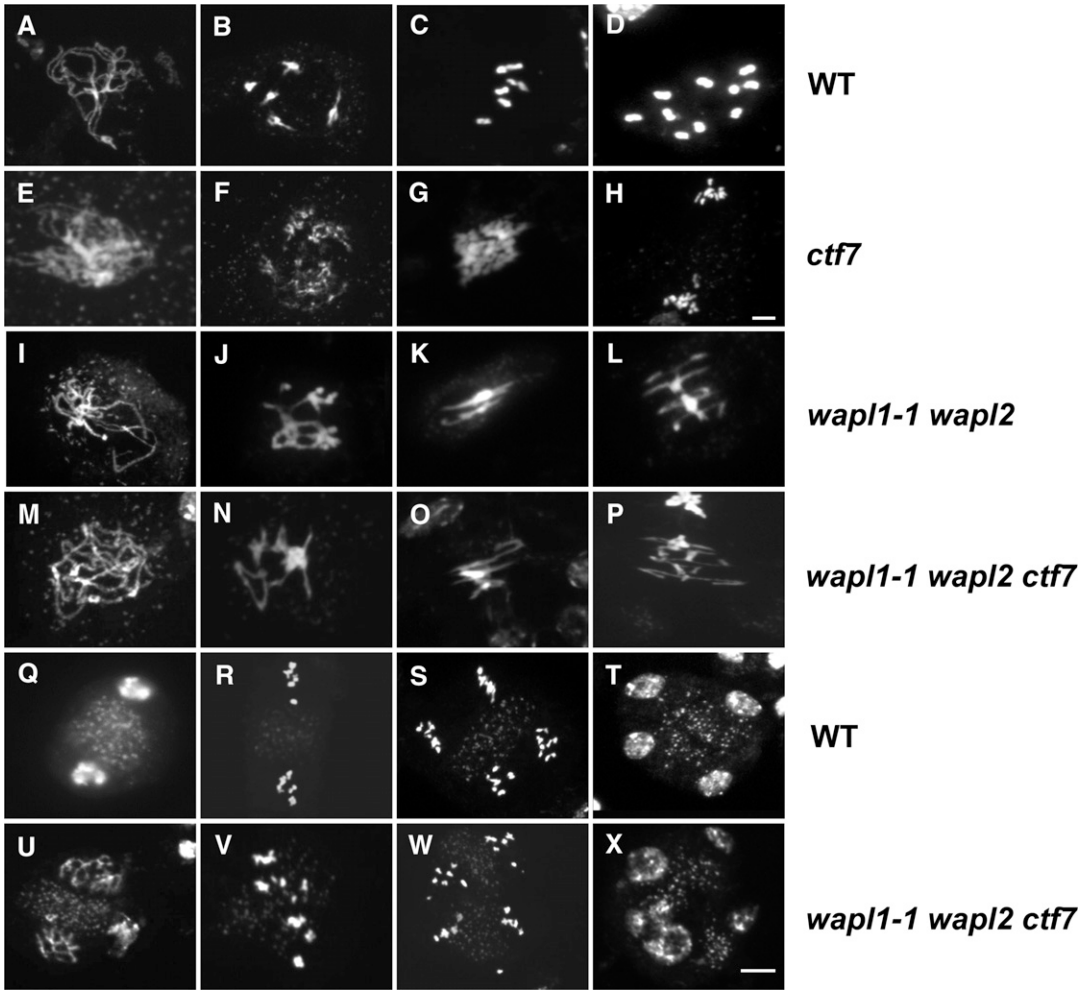

Figure 5. Arabidopsis *wapl1-1 wapl2 ctf7* Plants Exhibit Defects during Male Meiosis.

DAPI-stained chromosomes from male meiocytes of wild-type (**[A]** to **[D]** and **[Q]** to **[T]**), *ctf7* (**[E]** to **[H]**), *wapl1-1 wapl2* (**[I]** to **[L]**), and *wapl1-1 wapl2 ctf7* (**[M]** to **[P]** and **[U]** to **[X]**) plants are shown at pachytene (**[A]**, **[E]**, **[I]**, and **[M]**), diakinesis (**[B]**, **[F]**, **[J]**, and **[N]**), metaphase I (**[C]**, **[G]**, **[K]**, and **[O]**), anaphase I (**[D]**, **[H]**, **[L]**, and **[P]**), telophase I (**[Q]** and **[U]**), metaphase II (**[R]** and **[V]**), anaphase II (**[S]** and **[W]**), and telophase I/tetrad (**[T]** and **[X]**). Bars = 5 μm.

broken chromosomes during telophase I (Figure 5U). Most interphase II and metaphase II cells contained 20 or more chromosomes, indicating that centromere cohesion is prematurely lost, similar to the situation in *wapl1-1 wapl2* plants. Missegregation of chromosomes during meiosis II resulted in the formation of a mixture of tetrads and polyads (Figure 5X). Therefore, WAPL inactivation suppresses *ctf7* defects early in meiosis; however, the *wapl1-1 wapl2*-related defects observed from diplotene onwards are still present in triple mutant plants.

The *wapl1-1 wapl2* mutation results in the nonspecific association of centromeres (De et al., 2014). In order to determine if this is also the situation in *wapl1-1 wapl2 ctf7* plants, in situ hybridization was conducted using the 180-bp centromere (CEN) repeat as a probe. Meiocytes of *ctf7* plants typically contain 11 to 15 irregular CEN signals during leptotene and zygotene (Figures 6E and 6F). As *ctf7* meiocytes progress through meiosis I and II, the number of centromere signals increases, with 10 to 20 centromere signals typically observed from pachytene to diakinesis and twenty or more signals observed from metaphase I through meiosis II (Figures 6G and 6H). Centromere signals resembling those in the wild type (Figures 6A to 6D and 6Q to 6T) were observed throughout meiosis in ~50% of both *wapl1-1 wapl2* and *wapl1-1 wapl2 ctf7* meiocytes. The other half of the cells appeared normal during leptotene and early zygotene (Figures 6I and 6M), but were found to contain clusters of condensed CEN signals from late zygotene to diakinesis (Figures 6J, 6K, 6N, and 6O). Individual centromere signals were observed within the condensed chromatin at late diakinesis and metaphase I (Figures 6L and 6P). Some normal anaphase I cells were observed; however, more than 10 centromere signals were observed beginning at anaphase I in 80% of the *wapl1-1 wapl2 ctf7* meiocytes observed (n = 21), indicating that similar to the situation in *wapl1-1 wapl2*, centromere cohesion is lost prematurely or never properly formed in these cells. While a small number of cells proceed normally through meiosis, most cells contain missegregated chromosomes and chromosome fragments at telophase I (Figure 6V) and during meiosis II (Figures 6W and 6X; n = 17).

The effect of eliminating both WAPL and CTF7 on meiotic prophase was further investigated by examining the distribution of ASY1 (Armstrong et al., 2002) and ZYP1 (Higgins et al., 2005), which are distributed on chromatin and are essential for normal synapsis, on prophase chromosomes. Similar to the situation for *wapl1-1 wapl2* plants (De et al., 2014), no obvious differences were observed in ASY1 labeling between wild-type and *wapl1-1 wapl 2ctf7* meiocytes (Supplemental Figure 5A). ASY1 signals first appeared as diffuse foci on the univalent axes during late G2/early leptotene and then lined the axes of synapsed chromosomes during pachytene; from diplotene onward, ASY1 signals were not observed. ZYP1 signals also appeared normal in *wapl1-1 wapl2ctf7* meiocytes ($n = 64$). ZYP1 signals appeared as foci during leptotene, which then extend and coalesce during zygotene such that by pachytene, the ZYP1 signal extends along the lengths of the synapsed chromosomes (Supplemental Figure 5B).

The effect of inactivating both WAPL and CTF7 on meiotic cohesin distribution was determined by examining the distribution of cohesin protein SYN1 (Cai et al., 2003). In wild-type meiocytes, SYN1 shows a diffuse labeling pattern on the condensing chromosomes during early leptotene and decorates the developing chromosomal axes during late leptotene and zygotene, ultimately lining the axes of synapsed chromosomes from late zygotene to pachytene (Figures 7A and 7B). Arm cohesin is released from chromosomes during diplotene and diakinesis as the chromosomes condense (Figure 7C) and by pro-metaphase I, very little SYN1 is observed on the condensed chromosomes (Figure 7D).

The loading and distribution of SYN1 is severely affected in *ctf7-1* meiocytes (Bolaños-Villegas et al., 2013). SYN1 labeling is very weak and irregular during leptotene and zygotene (Figure 7E) and becomes progressively weaker as prophase progresses (Figures 7F to 7H). In contrast, cohesin labeling is normal in *wapl1-1 wapl2* plants during early stages of prophase I, with SYN1 labeling

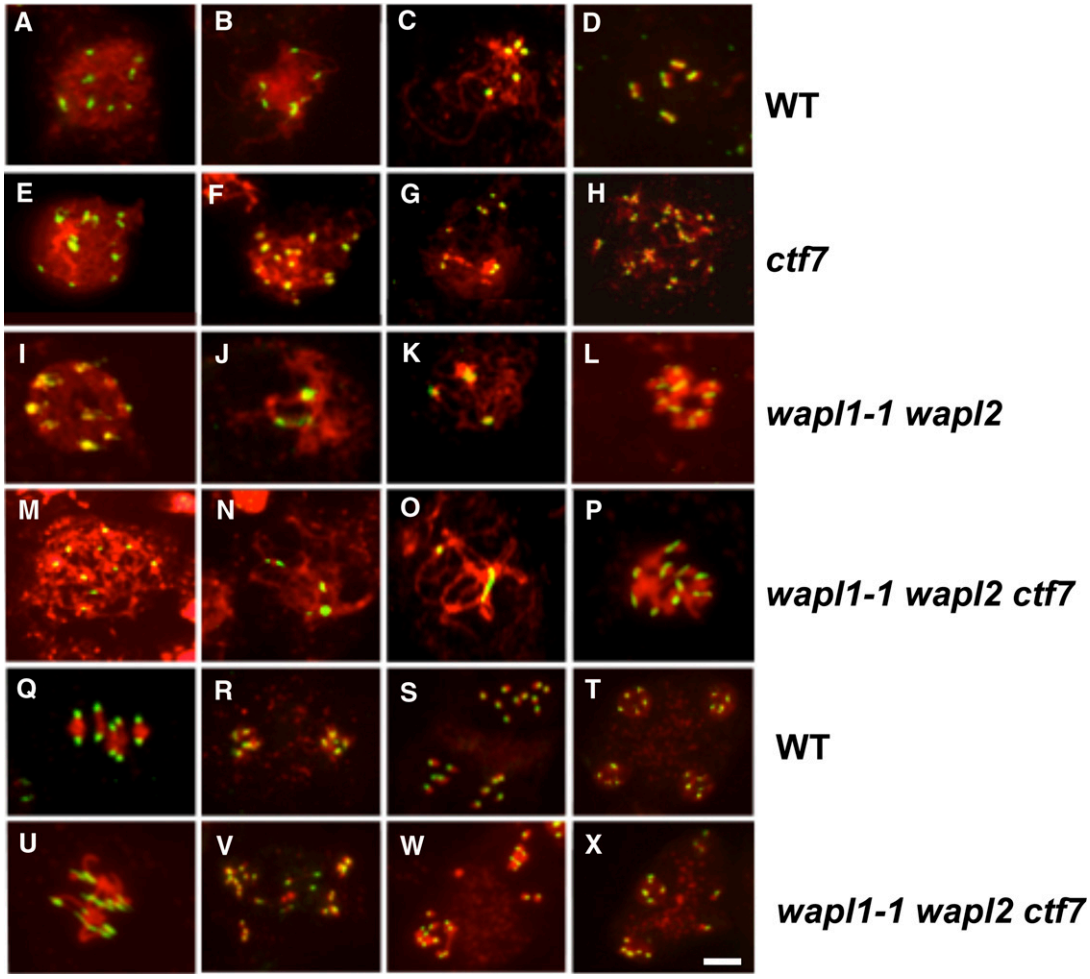

Figure 6. *wapl1-1 wapl2 ctf7* Male Meiocytes Exhibit Nonspecific Association of Centromeres.

FISH was conducted on male meiocytes from wild-type (**[A]** to **[D]** and **[Q]** to **[T]**), *ctf7* (**[E]** to **[H]**), *wapl1-1 wapl2* (**[I]** to **[L]**), and *wapl1-1 wapl2 ctf7* (**[M]** to **[P]** and **[U]** to **[X]**) plants with a centromere probe. DAPI-stained chromosomes are shown in red, and the centromere signal is shown in green. Cells are shown at leptotene (**[A]**, **[E]**, **[I]**, and **[M]**), zygotene (**[B]**, **[F]**, **[J]**, and **[N]**), pachytene (**[C]**, **[G]**, **[K]**, and **[O]**), diakinesis (**[D]**, **[H]**, **[L]**, and **[P]**), metaphase I **(Q)**, early anaphase I **(U)**, anaphase I (**[R]** and **[V]**), anaphase II (**[S]** and **[W]**), and telophase II (**[T]** and **[X]**). Bar = 5 μm.

the developing axes during leptotene (Figure 7I) and zygotene and completely lining the synapsed chromosomes at pachytene (Figure 7J). However, cohesin release from chromosome arms is delayed (Figure 7K) and strong SYN1 labeling of the chromosomes is consistently observed on metaphase I and early anaphase I chromosomes in *wapl1-1 wapl2* meiocytes (Figure 7L).

SYN1 labeling patterns were normal during early prophase in *wapl1-1 wapl2 ctf7* meiocytes. SYN1 exhibited diffuse nuclear labeling early, with the signal decorating the developing chromosomal axes beginning at early leptotene and extending into zygotene (Figure 7M). The protein lined the axes of paired chromosomes during late zygotene and pachytene (Figure 7N). While not as dramatic as the alterations in *wapl1-1 wapl2* plants, SYN1 release from the chromosomes during diplotene and diakinesis appeared to be delayed, with strong SYN1 signals observed on the chromosomes at diplotene and diakinesis (Figure 7O). However, the SYN1 signal was reduced during pro-metaphase/metaphase I, with little to no signal being observed by anaphase I (Figure 7P). Therefore, inactivation of both CTF7 and WAPL results in the normal association of SYN1 with the chromosomes early in meiosis, but only partially restores the prophase removal of cohesin.

The presence of fused microspores in tetrads of *wapl1-1 wapl2 ctf7* plants suggested that cytokinesis may also be altered. Therefore, spindle formation was analyzed and compared with the wild type (Figures 8A to 8F). Abnormalities in spindle organization were observed in ~80% of *wapl1-1 wapl2 ctf7* meiocytes ($n = 70$). The most common alteration observed during metaphase I was distorted spindles (Figure 8G), including spindle microtubules that passed over the chromosomes and cells that lacked a bipolar spindle altogether. During anaphase I and telophase I, the spindles were typically not well defined, and in ~30% of the meiocytes, chromosomes did not attach to the spindles (Figures 8H and 8I). During meiosis II, cells containing parallel spindles (Figure 8J; $n = 5$) or spindle microtubules that connected small individual groups of chromosomes were commonly observed (Figure 8K; $n = 5$). Abnormalities were also observed in the radial microtubule system of ~90% of the cells ($n = 24$) at telophase/tetrad stage (Figure 8L), which is consistent with the high percentage of aborted pollen in *wapl1-1 wapl2 ctf7* plants.

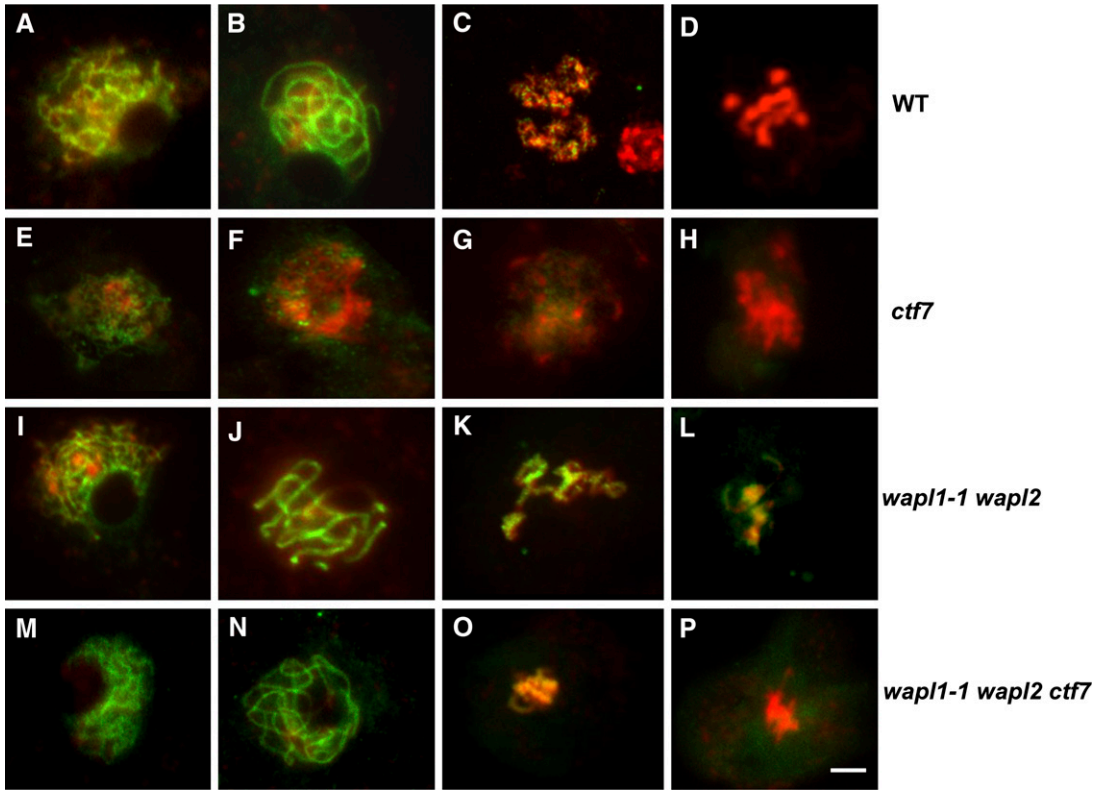

Figure 7. Cohesin Establishment Is Recovered in *wapl1-1 wapl2 ctf7* Meiocytes.

Meiotic spreads of wild-type (**[A]** to **[D]**), *ctf7* (**[E]** to **[H]**), *wapl1-1 wapl2* (**[I]** to **[L]**), and *wapl1-1 wapl2 ctf7* (**[M]** to **[P]**) plants were prepared and stained with anti-SYN1 antibody (green) and propidium iodide (red). Meiocytes in wild-type, *wapl1-1 wapl2*, and the *wapl1-1 wapl2 ctf7* plants exhibited similar SYN1 staining patterns from leptotene to pachytene. The ctf7 mutant did not exhibit a clear SYN1 signal during leptotene **(E)**, zygotene **(F)**, pachytene **(G)**, or diakinesis **(H)**. In wild-type meiocytes, SYN1 is removed from the arms of chromosomes during diplotene and diakinesis **(C)**; it was not detectable during pro-metaphase I **(D)**. Strong SYN1 signals are detectable in *wapl1-1 wapl2* during diakinesis, metaphase, and anaphase a (**[J]** to **[L]**). SYN1 signals resemble the wild type on *wapl1-1 wapl2 ctf7* chromosomes during leptotene and pachytene (**[M]** and **[N]**). During diplotene, condensed diakinesis **(O)**, and late diakinesis/metaphase, SYN1 signals remained strong. Little to no SYN1 signal is detected by metaphase/anaphase I **(P)**. Bar = 5 μm.

DISCUSSION

In this study, we characterized the interaction between Arabidopsis CTF7 and WAPL by conducting a detailed analysis of *wapl1-1 wapl2 ctf7* plants. Inactivation of CTF7/ECO1 typically results in lethality in animals, plants, and yeast (Skibbens et al., 1999; Vega et al., 2005; Jiang et al., 2010). However, for reasons that are not yet understood, *ctf7* plants can be obtained at low frequencies; the plants are dwarf, exhibit severe developmental abnormalities, and are completely sterile (Bolaños-Villegas et al., 2013). Inactivation of WAPL results in lethality in *Drosophila melanogaster*, nematodes (*Caenorhabditis elegans*), and animal cells (Vernì et al., 2000; Kamath et al., 2003; Tedeschi et al., 2013); however the growth of *wpl1/rad61* yeast mutants is indistinguishable from the wild type (Bennett et al., 2001). Similar to the situation in yeast, WAPL inactivation in Arabidopsis has very little effect on growth and development. *wapl1-1 wapl2* plants appear relatively normal but exhibit defects in both male and female meiosis (De et al., 2014). Also similar to the situation in yeast (Rolef Ben-Shahar et al., 2008; Unal et al., 2008; Zhang et al., 2008; Rowland et al., 2009; Sutani et al., 2009), inactivation of *WAPL* suppresses the lethality associated with *ctf7* mutations in Arabidopsis (De et al., 2014). *wapl1-1 wapl2 ctf7* plants are obtained at expected rates, display normal growth and development, and produce small numbers of viable seed. Therefore, inactivation of *WAPL* is able to suppress the growth defects associated with CTF7 inactivation and reduce the severity of defects in generative cells.

Proper Cohesin Levels Are Essential for Meiotic Chromosome Segregation

While WAPL inactivation can restore some fertility to *ctf7* plants, the fertility of *wapl1-1 wapl2 ctf7* plants is significantly lower than that of *wapl1-1 wapl2* plants. *ctf7* plants exhibit a dramatic reduction in chromosome-bound cohesin that results in defects in meiotic chromosome condensation and cohesion during leptotene and zygotene followed by a failure of homologous chromosomes to properly align and synapse during zygotene and pachytene (Bolaños-Villegas et al., 2013). In contrast, early stages of meiosis are relatively normal in *wapl1-1 wapl2* plants (De et al., 2014). Rather, inactivation of WAPL results in the prolonged association of cohesin with chromosomes during diplotene and diakinesis, which results in condensation defects and a failure of the chromosomes to resolve, resulting in large intertwined chromatin masses that do not separate properly (De et al., 2014). Meiosis in *wapl1-1 wapl2 ctf7* plants is similar to that observed in *wapl1-1 wapl2* plants. No obvious alterations are observed in sister chromatid cohesion, chromosome-bound cohesin levels, chromosome condensation, or the pairing of homologous chromosomes during leptotene, zygotene, and pachytene. While less severe than the situation in *wapl1-1 wapl2* plants, triple mutant plants exhibit delayed cohesin removal, which results in diplotene chromosomes that fail to desynapse properly. Therefore, *WAPL* inactivation is able to suppress *ctf7*-associated cohesin defects early in meiotic prophase, while the *ctf7* mutation only had a minor effect on *wapl*-associated alterations later in prophase.

WAPL appears to play multiple roles in the cell, which can vary between organisms and between mitosis and meiosis (Haarhuis et al., 2014). Studies in yeast and animal cells have shown that WAPL in conjunction with PDS5 plays an important role in regulating the reversible binding of cohesin to chromosomes (Bernard et al., 2008; Sutani et al., 2009; Chan et al., 2012; Lopez-Serra et al., 2013). Prior to DNA replication, WAPL either opens or maintains an open conformation of the cohesin ring at the junction between the SMC3 ATPase domain and the SCC1 N-terminal WHD (Chatterjee et al., 2013; Ouyang et al., 2013). During DNA replication, WAPL-dependent antiestablishment activity is blocked through Eco1/Ctf7-dependent acetylation of SMC3, which results in stable cohesin binding to the chromosomes and the establishment of cohesion (Vernì et al., 2000; Siomos et al., 2001; Bernard et al., 2008; Shintomi and Hirano, 2009; Cunningham et al., 2012). Our observation that meiotic chromosomes in *wapl1-1 wapl2 ctf7* plants resemble the wild type from leptotene through pachytene indicates that CTF7 is essential for meiotic cohesion establishment only in the presence of *WAPL*. Therefore, one role of *CTF7* is to antagonize WAPL activity prior to DNA replication.

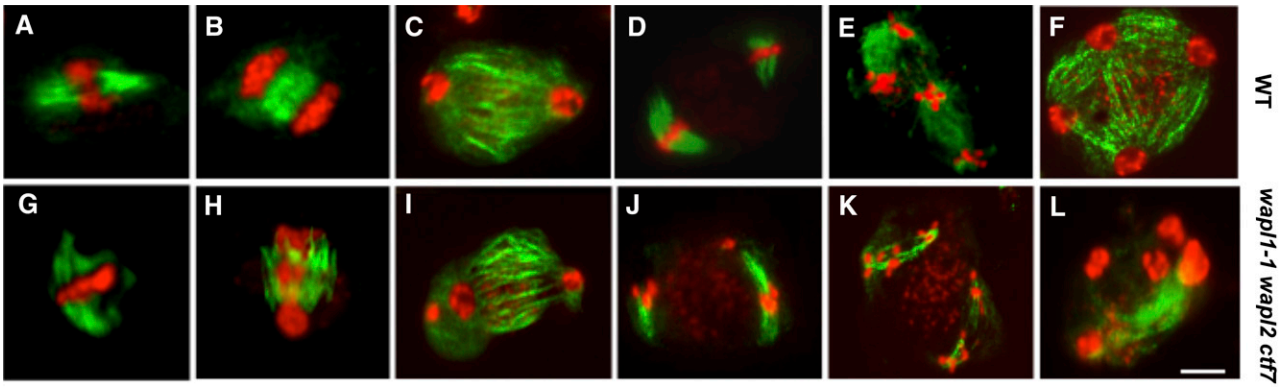

Figure 8. The Radial Microtubule System Is Disrupted in *wapl1-1 wapl2 ctf7*Plants.

Spindles of male meiocytes from wild-type (**[A]** to **[F]**) and *wapl1-1 wapl2 ctf7* (**[G]** to **[L]**) plants were stained using anti-β-tubulin antibody (green). DNA was counterstained with propidium iodide (red). Male meiocytes are shown at metaphase I (**[A]** and **[G]**), anaphase I (**[B]** and **[H]**), telophase I (**[C]** and **[I]**), metaphase II (**[D]** and **[J]**), anaphase II (**[E]** and **[K]**), and telophase II/tetrad stages (**[F]** and **[L]**). Bars = 10 μm.

Wapl is also involved in the nonproteolytic removal of cohesin from mitotic chromosome arms during the prophase pathway in vertebrate cells (Chatterjee et al., 2013; Ouyang et al., 2013). Plk1 and Aurora B phosphorylate multiple sites on sororin, which leads to its disassociation from acetylated cohesin complexes and subsequent ring opening of the cohesin complex by Wapl (Hauf et al., 2005; Nishiyama et al., 2010; Nasmyth, 2011). Similar to the situation in somatic cells of vertebrates, meiosis in Arabidopsis includes the prophase removal of cohesin (Cai et al., 2003), which is dependent on the presence of WAPL (De et al., 2014). However, a sororin ortholog has not yet been identified in Arabidopsis, suggesting that acetylation of SMC3 may directly interfere with WAPL binding in plants.

WAPL also plays a role in regulating chromosome condensation in yeast, animal, and plant cells. In yeast, RAD51 deletion has been shown to suppress *pds5* and *ctf7* condensation defects (Tong and Skibbens, 2015). This led to the suggestion that Pds5 and Ctf7/Eco1 promote condensation through a common WAPL-mediated mechanism regulated by Rad51 (Tong and Skibbens, 2015). Mouse cells depleted for Wapl contain partially condensed chromosomes with regions of hypercondensed heterochromatin (Tedeschi et al., 2013). It is has been suggested that this could be due in part to a failure to remove catenates during late prophase. Catenates are maintained by cohesion, and the prophase removal of arm cohesion is required for the timely deconcatenation of chromosomes in yeast (Wang et al., 2010; Farcas et al., 2011). We show here that the loss of CTF7 reduced/eliminated early meiotic chromosome condensation defects associated with WAPL inactivation (De et al., 2014) but did not suppress the chromosome condensation and centromere association defects late in prophase. This suggests that early chromosome condensation events involve removal of CTF7-stabilized cohesin by WAPL but that chromosome resolution and disassociation of centromeres does not depend on CTF7-stabilized cohesin.

Consistent with the suggestion that WAPL may function beyond its role as an CTF7 antagonist is the observation that sister chromatid cohesion is prematurely lost at the centromeres of both *wapl1-1 wapl2* (De et al., 2014) and *wapl1-1 wapl2 ctf7* meiocytes starting at telophase I (Figure 6). Likewise, alterations in spindle morphology and microtubule attachment are common in meiocytes of both *wapl1-1 wapl2* and *wapl1-1 wapl ctf7* plants. WAPL depletion can result in the distribution of the chromosome passenger complex along mitotic chromosome arms and its depletion at the centromeres, resulting in altered microtubule attachment and erroneous microtubule-kinetochore attachments and errors in mitotic chromosome segregation (van der Waal et al., 2012; Haarhuis et al., 2013). The erroneous microtubule-kinetochore attachment and alterations in chromosome condensation and decatenation observed in *wapl1-1 wapl ctf7* plants are consistent with possible alterations in centromeric cohesin structure. The observation that the alterations are independent of CTF7 inactivation suggests that a second form of cohesin may exist that is not stabilized by CTF7. It is also possible that WAPL may regulate the binding of condensin and/or affect chromatin structure in some as of yet unknown way. While additional experiments are required to further define the roles of WAPL in plants, it is clear that WAPL plays roles during meiosis that are at least in part independent of its role in regulating CTF7-stabilized cohesin.

CTF7 and WAPL Are Essential for Embryo Development, but Not Normal Plant Growth and Development

As shown here, plant reproduction is very sensitive to the level and distribution of cohesin and requires both CTF7 and WAPL for meiosis. In contrast, vegetative growth is not affected in *wapl1-1 wapl2 ctf7* plants. This is surprising because many of the somatic cell defects identified in the leaves of *ctf7* plants are still present in *wapl1-1 wapl2 ctf7* plants. For example, similar to *ctf7*, leaf samples of *wapl1-1 wapl2* and *wapl1-1 wapl2 ctf7-1* plants contain increased numbers of polyploid cells and elevated levels of cells exhibiting apparent aneuploidy (Figure 2). Likewise, reduced DNA DSB repair rates and high levels of chromocenter decondensation were observed in leaf nuclei of *ctf7*, *wapl1-1 wapl2*, and *wapl1-1 wapl2 ctf7* plants (Figure 2). These results indicate that while deletion of CTF7 and WAPL either alone or together results in defects in cell cycle progression, DNA repair, and altered DNA content, these alterations are tolerated by the plant under normal growth conditions.

The presence of leaf cells with altered DNA content in *ctf7*, *wapl1-1 wapl2*, and *wapl1-1 wapl2 ctf7* plants suggested that all three lines may exhibit alterations in mitosis. However, while mitotic alterations, including the presence of "sticky metaphase chromosomes," chromosome bridges, lagging chromosomes, and chromosome fragments at telophase were observed in 80% of *ctf7* (Bolaños-Villegas et al., 2013) and 20% of *wapl1-1 wapl2* root tip cells (De et al., 2014), no mitotic alterations were detected in the root tips of *wapl1-1 wapl2 ctf7* plants (Supplemental Figure 2A). This raises the possibility that mitotic cohesion is regulated differently in roots and leaves and/or that mitosis in root cells is less sensitive than leaf cells to alterations in cohesion. While we cannot rule out these possibilities, we suggest that mitosis in leaf cells is likely normal and that the apparent aneuploidy is due to a general increase in genomic instability in the mutants and not to chromosome segregation alterations during mitosis. It is well established that cohesin complexes play an important role in DNA repair (Dorsett and Merkenschlager, 2013) and that inactivation of WAPL results in genomic instability (Haarhuis et al., 2013). Loss of *WPL1* activity in yeast has been linked to interallelic recombination, chromosomal amplification, and aneuploidy at rates 17-fold higher than wild-type colonies (Covo et al., 2014a, 2014b). Likewise, point mutations in human, mouse, and yeast CTF7/Eco1 orthologs result in hypersensitivity to DNA damaging agents (van der Lelij et al., 2009; Lu et al., 2010; Whelan et al., 2012). While further experiments are required to directly analyze mitosis in leaf cells, the conclusion that mitosis is normal in *wapl1-1 wapl2 ctf7* plants is consistent with our results showing that inactivation of CTF7 and WAPL together suppresses the mitotic defects associated with either of the individual mutations in root cells.

Many of the growth differences between *ctf7* and *wapl1-1 wapl2 ctf7* plants can be explained by differences in the level of mitotic alterations observed between the two lines. For example, in the absence of WAPL, cohesin is not removed normally from the chromosomes, low frequency (20%) mitotic alterations occur, and plant growth is slower than the wild type. In the absence of CTF7, the WAPL-catalyzed removal of cohesin during prophase is not antagonized, causing extensive mitotic alterations (~80% in *ctf7* plants), resulting in plants that are dwarf and exhibit

developmental alterations. Inactivation of the CTF7/WAPL-regulated cohesin system by inactivating both CTF7 and WAPL results in normal mitosis and plant growth. Therefore, the CTF7/WAPL-regulated cohesin pathway is dispensable for mitosis under normal growth conditions. This raises the possibility that plants may contain an alternate pathway to regulate sister chromatid cohesion during mitosis that is independent of CTF7 and WAPL. In support of this, a CTF7-independent cohesin establishment pathway has been reported in budding yeast (Borges et al., 2013). It is also possible that a cohesin-independent mechanism exists that enables the bipolar attachment and segregation of mitotic chromosomes, as has been reported for budding yeast (Guacci and Koshland, 2012). Further studies are clearly required to determine if in fact plants contain an alternate pathway to regulate mitotic cohesin and to better understand the roles CTF7 and WAPL play in mitosis and chromatin structure.

While normal plant growth and development does not require the CTF7/WAPL-regulated cohesin system, it is required for embryo development. *ctf7* plants are unable to produce viable seed, while embryo defects are observed in 23 and 7% of the developing seeds in *wapl1-1 wapl2* (De et al., 2014) and *wapl1-1 wapl2 ctf7*plants, respectively. The embryo defects, which are generally similar in the two mutant lines, could arise from several of the cohesion-associated alterations we have identified. Mitotic alterations and/or chromosome instability in zygotes or during early embryo development is expected to have severe consequences on subsequent rounds of cell division that could arrest embryo development. Likewise, alterations in chromatin condensation and/or structure could affect gene expression patterns that are critical for embryo development. Cohesins have been shown to play a role in transcriptional regulation in several organisms (Peric-Hupkes and van Steensel, 2008; Dorsett, 2011; Ball et al., 2014). They facilitate long-distance DNA interactions (Dorsett and Merkenschlager, 2013) and have been shown to affect long-range interactions between binding sites of the transcriptional repressor CTCF in a number of genes in animal cells (Bonora et al., 2014). Consistent with this, alterations in cohesin protein levels can result in tissue-specific alterations in transcript levels for a number of genes in Arabidopsis (this study; Yuan et al., 2012; Bolaños-Villegas et al., 2013; Liu and Makaroff, 2015). For example, transgenic plants expressing a pro35S:AtCTF7ΔB construct and *ctf7* plants contain elevated levels of transcripts for epigenetically regulated transposable elements, including *MU1*, *COPIA 28*, and *solo LTR*, and alterations in transcript levels of several small interfering RNA-associated genes (Bolaños-Villegas et al., 2013; Liu and Makaroff, 2015). Therefore, it is possible that inactivation of CTF7 and/or WAPL results in chromatin conformational changes that alter transcriptional patterns and cause the embryo arrest we observe. Finally, the tissue-specific and developmentally regulated differences in transcriptional patterns observed here suggest that cohesins may play a role in regulating developmentally related chromatin conformation in plants. Detailed transcriptional profiling and chromatin conformational analyses of developing embryos and developmentally staged tissues in different cohesin mutant backgrounds will be required to investigate this possibility and to better understand how cohesins modulate chromatin conformation and influence transcription in plants.

METHODS

Plant Material and Growth Conditions

The *Arabidopsis thaliana* Columbia ecotype was used for crossing, transcript analysis, and microscopy studies. Plants were grown in Metro-Mix 200 soil (Scotts-Sierra Horticulture Products) or on germination plates (Murashige and Skoog [MS]; Caisson Laboratories) in a growth chamber at 22°C with a 16-h-light/8-h-dark cycle. The leaves were collected from rosette-stage plants grown on soil and used for DNA isolation and genotyping. Approximately 24 d after germination, flower buds were collected and staged for microscopy studies. For transcript analysis, all samples were harvested, frozen in liquid N_2, and stored at −80°C until needed.

Chromosome Analysis and Immunolocalization

Male meiotic chromosome spreads were performed on floral buds fixed in Carnoy's fixative (ethanol:chloroform:acetic acid: 6:3:1, v/v) and prepared as described previously (Ross et al., 1996). Chromosomes were stained with DAPI and observed with an Olympus BX51 epifluorescence microscope system. Images were captured using a Spot camera system and processed using Adobe Photoshop. Mitosis was studied in root tips. Arabidopsis seeds were sterilized and plated on MS agar plates. Root tips were harvested from 7-d-old seedlings and fixed as previously described (Ross et al., 1996).

Immunolocalization of cohesin proteins and β-tubulin was performed on paraformaldehyde-fixed cells as previously described (Yang et al., 2009). Meiotic stages were assigned based on the chromosome structure and cell morphology as well as the developmental stage of the surrounding anther cells. Primary antibodies to Arabidopsis proteins used at 1:500 dilutions have been described (Cai et al., 2003; Lam et al., 2005). Mouse anti-β-tubulin antibody (#E7; Developmental Studies Hybridoma Bank) was used at 1:100 dilutions. The slides were incubated overnight at 4°C and then washed for 2 h with eight changes of wash buffer. The slides were incubated overnight at 4°C with Alexa 488-labeled goat anti-rabbit (#A-11008; Thermo Fisher Scientific) secondary antibody (1:500) or with Alexa Fluor 594-labeled goat anti-mouse (#A-11005; Thermo Fisher Scientific) secondary antibody (1:500), washed, and then stained with DAPI.

Fluorescence in situ hybridization (FISH) was conducted on meiocytes from inflorescences fixed in Carnoy's solution for 1 h at room temperature after replenishing the fixative. FISH was performed with the 180-bp centromere repeat as a probe on meiotic spreads as previously described (Fransz et al., 1996; Caryl et al., 2000) with the following modification. Samples were treated with a solution of freshly prepared 70% formamide in 2× SSC for 2 min at 80°C and dehydrated through a graded ethanol series (70, 90, and 100%) for 5 min at −20°C. The slides were then dried at room temperature before adding the probe. The 180-bp pericentromeric repeat (Martinez-Zapater et al., 1986) was amplified, purified, labeled with Roche High Prime fluorescein, and then used as a probe at a concentration of 5 μg mL^{-1}. Telomere repeat sequences were detected by hybridization with a 5′-end fluorescein isothiocyanate-labeled oligonucleotide probe $(CCCTAAA)_6$ at 5 μg mL^{-1}. Slides were counterstained with DAPI and observed as describe above.

Gene Expression Analyses

Total RNA was extracted from stems, buds, roots, leaves, and siliques of wild-type, *wapl1-1 wapl2*, and *wapl1.2 wapl2 ctf7-1* plants to measure *WAPL* transcript levels. Total RNA was extracted with the Plant RNeasy Mini kit (Qiagen), treated with Turbo DNase I (Thermo Fisher Scientific), and used for cDNA synthesis with the First Strand cDNA Synthesis Kit (Roche). RT-qPCR was performed with SYBR-Green PCR Mastermix (Clontech). Amplification was monitored on a CFX system (Bio-Rad). Expression was normalized against the *β-tubulin-2*. At least three biological replicates

were sampled, with two technical replicates for each sample. Primers used in this study are presented in Supplemental Table 1.

Analysis of Female Gametophyte Development and Embryo Development

To determine the phenotype of embryos, whole-mount clearing was used (Herr, 1971; Vielle-Calzada et al., 2000). Hoyer's solution containing lactic acid:chloral hydrate:phenol:clove oil:xylene (2:2:2:2:1, w/w) was used as a clearing agent on the dissected siliques from wild-type and mutant plants. Samples were observed with an Olympus BX51 microscope equipped with differential interference contrast optics. Female gametophyte analysis was performed as previously described (Siddiqi et al., 2000).

Flow Cytometry

Cells from the first true leaves of 9-d-old seedlings were isolated and stained with a CyStain PI Absolute P Kit (Partec), and the resulting suspension was run through a MoFlo XDP Laser Cell Sorter machine (Beckman Coulter). Results were analyzed with Summit V5 3.1 software (Beckman Coulter) from at least three different biological samples and three technical repeats. Analysis was performed with at least 10,000 nuclei per sample. The relative frequencies of nuclei populations with intermediate ploidy values were estimated using the gating analysis tool of the Summit V5 3.1 software.

Neutral Comet Assay for DNA Repair

DNA DSB repair was measured using a Comet assay as previously described (Bolaños-Villegas et al., 2013). This assay has been used in Arabidopsis as a reliable method to quantify DNA repair kinetics in response to chemical and environmental agents that cause DNA damage (Luo et al., 2012; Nezames et al., 2012). The assay is prone to saturation and requires prior calibration of doses and the careful standardization of experimental conditions to maintain background DNA damage at a minimum (Collins et al., 2008). Mutant and wild-type plants were grown on MS plates for 8 d and then transferred to 0.5× MS liquid medium containing Mitomycin C (50 μg/mL). Short treatments (1 to 2 h.) with Mitomycin C have been shown to be effective in generating DNA DSBs (Bohmdorfer et al., 2011). After incubation for 2 h in the dark, the plants were washed three times with distilled water and incubated for 1 h in liquid 0.5× MS medium without Mitomycin C. Leaves were excised, prepared, and then processed with a Trevigen CometAssay Kit (Trevigen) according to the manufacturer's instructions and published procedures (Collins et al., 2008; Kozak et al., 2009). Peroxide was used as a positive control for the oxidation status of the cells (Collins, 2014). Slides were observed under an Olympus BX51 epifluorescence microscope with the fluorescein isothiocyanate filter. Comets were analyzed with TriTek Comet Score freeware (version 1.5; TriTek). At least 300 nuclei per line were analyzed. Damage remaining after a given repair time (*tx*) was estimated according to Kozak et al. (2009). Results were obtained from at least three different biological samples, with three technical repeats and a negative control for each line.

Immunolocalization on Leaf Nuclei

Chromocenter condensation was investigated by performing immunolocalization with anti-H3K9me2 antibody (#07-441; Millipore) as described (Soppe et al., 2002; Moissiard et al., 2012), with minor modifications. Briefly, leaves were fixed for 40 min in 4% formaldehyde in Tris buffer, chopped in 400 μL lysis buffer (15 mM Tris, pH 7.5, 2 mM EDTA, 0.5 mM spermine, 80 mM KCl, 20 mM NaCl, and 0.1% Triton X-100) and filtered through a 35-μm cell membrane. Six microliters of nuclei suspension was added to 50 μL of sorting buffer (100 mM Tris, pH 7.5, 50 mM KCl, 2 mM $MgCl_2$, 0.05% Tween 20, and 20.5% sucrose) and released on poly-L-lysine-coated slides. Samples were allowed to air dry for 2 h, postfixed in 4% formaldehyde in PBS for 40 min, washed for 30 min in 1× PBS, 1% Triton X-100, and incubated for 1 h in 200 μL of blocking buffer (1× PBS, 5% BSA, 0.1% Tween 20, and 1 mM EDTA) at 37°C. Nuclei were then incubated at 4°C overnight in 50 μL of anti-H3K9me2 antibody (1:50). Slides were washed in 1× PBS 0.1% Tween 20 and incubated with 50 μL Alexa Fluor 488 goat anti-rabbit secondary antibody (1:200) (Invitrogen) for 90 min at 37°C. Slides were washed and nuclei were stained with Vectashield mounting media with DAPI (30 μL per slide) (Vector Labs). Nuclei were analyzed at 100× magnification under a Z1 Axio observer microscope (Zeiss). Nuclei were obtained from at least three different biological samples, and at least 300 nuclei per line were scored.

Accession Numbers

Sequence data from this article can be found in the GenBank/EMBL libraries under the following accession numbers: ATM (At3g48190), ATR (At5g40820), BRCA1 (At4g21070), BRCA2B (At5g01630), CDC45 (At3g25100), *CTF7*/*ECO1* (AT4G31400), CYCB1;1 (At4g37490), DMC1 (At3g22880), PARP2 (At4g02390), RAD51 (At5g20850), SMC1 (At3g54670), SMC3 (At2g27170), TOPOII-α (At3g23890), *WAPL1* (AT1G11060), and *WAPL2* (AT1G61030).

Supplemental Data

Supplemental Figure 1. Flow cytometry profiles from roots of the wild type, *ctf7-1*, *wapl1-1 wapl2*, and *wapl1-1 wapl2 ctf7*.

Supplemental Figure 2. Cohesion establishment and release are normal in *wapl1-1 wapl1 ctf7* root tips.

Supplemental Figure 3. Comet images of leaf nuclei from 9-d-old seedlings from the wild type, *ctf7*, *wapl1-1 wapl2*, and *wapl1-1 wapl2 ctf7*.

Supplemental Figure 4. *wapl1-1 wapl2 ctf7* and *wapl1-1 wapl2* exhibit developmental differences in transcript levels for DNA repair genes.

Supplemental Figure 5. The distribution of synaptonemal complex and meiotic chromosome axis proteins is normal in *wapl1-1 wapl2 ctf7* meiocytes.

Supplemental Table 1. Primers used in this study.

ACKNOWLEDGMENTS

We thank Su-Hsin Huang for assistance in flow cytometry analysis (Flow Cytometry Analysis Laboratory, Academia Sinica), Mei-Jane Fang for assistance during use of the a Z1 Axio observer microscope (Plant Cell Biology Core Laboratory, Academia Sinica), and Sunny Lo Wan-Sheng (Institute of Plant and Microbial Biology, Academia Sinica) for kindly sharing anti-H3K9Me2 antibody. We also thank Hong Ma and Yingxiang Wang (School of Life Sciences, Fudan University) for providing antibody to ASY1 and ZYP1. This work was supported by a grant (MCB0718191) to Christopher A. Makaroff from the National Science Foundation, research grants from the Academia Sinica (Taiwan), the National Science and Technology Program for Agricultural Biotechnology (NSTP/AB, 098S0030055-AA, Taiwan), and the National Science Council (99-2321-B-001-036-MY3) to G.-Y.J. and by a study abroad contract to P.B.-V. from the University of Costa Rica.

AUTHOR CONTRIBUTIONS

K.D., P.B.-V., and C.A.M. designed the research. K.D., P.B.-V., S.M., X.Y., and G.H. performed the research. K.D., P.B.-V., X.Y., G.-Y.J., and C.A.M. analyzed data. K.D. and C.A.M. wrote the article.

Received September 8, 2015; revised January 6, 2016; accepted January 21, 2016; published January 26, 2016.

REFERENCES

Anderson, D.E., Losada, A., Erickson, H.P., and Hirano, T. (2002). Condensin and cohesin display different arm conformations with characteristic hinge angles. J. Cell Biol. **156:** 419–424.

Armstrong, S.J., Caryl, A.P., Jones, G.H., and Franklin, F.C. (2002). Asy1, a protein required for meiotic chromosome synapsis, localizes to axis-associated chromatin in Arabidopsis and Brassica. J. Cell Sci. **115:** 3645–3655.

Arumugam, P., Nishino, T., Haering, C.H., Gruber, S., and Nasmyth, K. (2006). Cohesin's ATPase activity is stimulated by the C-terminal Winged-Helix domain of its kleisin subunit. Curr. Biol. **16:** 1998–2008.

Ball, A.R., Jr., Chen, Y.-Y., and Yokomori, K. (2014). Mechanisms of cohesin-mediated gene regulation and lessons learned from cohesinopathies. Biochim. Biophys. Acta **1839:** 191–202.

Bennett, C.B., Lewis, L.K., Karthikeyan, G., Lobachev, K.S., Jin, Y.H., Sterling, J.F., Snipe, J.R., and Resnick, M.A. (2001). Genes required for ionizing radiation resistance in yeast. Nat. Genet. **29:** 426–434.

Bernard, P., Schmidt, C.K., Vaur, S., Dheur, S., Drogat, J., Genier, S., Ekwall, K., Uhlmann, F., and Javerzat, J.P. (2008). Cell-cycle regulation of cohesin stability along fission yeast chromosomes. EMBO J. **27:** 111–121.

Bohmdorfer, G., Schleiffer, A., Brunmeir, R., Ferscha, S., Nizhynska, V., Kozak, J., and Schweizer, D. (2011). GMI1, a structural-maintenance-of-chromosomes-hinge domain-containing protein, is involved in somatic homologous recombination in Arabidopsis. Plant J. **67:** 420–433.

Borges, V., Smith, D.J., Whitehouse, I., and Uhlmann, F. (2013). An Eco1-independent sister chromatid cohesion establishment pathway in *S. cerevisiae*. Chromosoma **122:** 121–134.

Bolaños-Villegas, P., Yang, X., Wang, H.J., Juan, C.T., Chuang, M.H., Makaroff, C.A., and Jauh, G.Y. (2013). Arabidopsis *CHROMOSOME TRANSMISSION FIDELITY 7* (*AtCTF7/ECO1*) is required for DNA repair, mitosis and meiosis. Plant J. **75:** 927–940.

Bonora, G., Plath, K., and Denholtz, M. (2014). A mechanistic link between gene regulation and genome architecture in mammalian development. Curr. Opin. Genet. Dev. **27:** 92–101.

Buonomo, S.B.C., Clyne, R.K., Fuchs, J., Loidl, J., Uhlmann, F., and Nasmyth, K. (2000). Disjunction of homologous chromosomes in meiosis I depends on proteolytic cleavage of the meiotic cohesin Rec8 by separin. Cell **103:** 387–398.

Cai, X., Dong, F., Edelmann, R.E., and Makaroff, C.A. (2003). The Arabidopsis SYN1 cohesin protein is required for sister chromatid arm cohesion and homologous chromosome pairing. J. Cell Sci. **116:** 2999–3007.

Caryl, A.P., Armstrong, S.J., Jones, G.H., and Franklin, F.C.H. (2000). A homologue of the yeast *HOP1* gene is inactivated in the *Arabidopsis* meiotic mutant *asy1.* Chromosoma **109:** 62–71.

Chan, K.L., Roig, M.B., Hu, B., Beckouët, F., Metson, J., and Nasmyth, K. (2012). Cohesin's DNA exit gate is distinct from its entrance gate and is regulated by acetylation. Cell **150:** 961–974.

Chatterjee, A., Zakian, S., Hu, X.W., and Singleton, M.R. (2013). Structural insights into the regulation of cohesion establishment by Wpl1. EMBO J. **32:** 677–687.

Collins, A.R. (2014). Measuring oxidative damage to DNA and its repair with the comet assay. Biochim. Biophys. Acta **1840:** 794–800.

Collins, A.R., Oscoz, A.A., Brunborg, G., Gaivão, I., Giovannelli, L., Kruszewski, M., Smith, C.C., and Stetina, R. (2008). The comet assay: topical issues. Mutagenesis **23:** 143–151.

Covo, S., Chiou, E., Gordenin, D.A., and Resnick, M.A. (2014a). Suppression of allelic recombination and aneuploidy by cohesin is independent of Chk1 in *Saccharomyces cerevisiae*. PLoS One **9:** e113435.

Covo, S., Puccia, C.M., Argueso, J.L., Gordenin, D.A., and Resnick, M.A. (2014b). The sister chromatid cohesion pathway suppresses multiple chromosome gain and chromosome amplification. Genetics **196:** 373–384.

Cunningham, M.D., Gause, M., Cheng, Y., Noyes, A., Dorsett, D., Kennison, J.A., and Kassis, J.A. (2012). Wapl antagonizes cohesin binding and promotes Polycomb-group silencing in Drosophila. Development **139:** 4172–4179.

De, K., Sterle, L., Krueger, L., Yang, X., and Makaroff, C.A. (2014). *Arabidopsis thaliana* WAPL is essential for the prophase removal of cohesin during meiosis. PLoS Genet. **10:** e1004497.

Dorsett, D. (2011). Cohesin: genomic insights into controlling gene transcription and development. Curr. Opin. Genet. Dev. **21:** 199–206.

Dorsett, D., and Merkenschlager, M. (2013). Cohesin at active genes: a unifying theme for cohesin and gene expression from model organisms to humans. Curr. Opin. Cell Biol. **25:** 327–333.

Farcas, A.M., Uluocak, P., Helmhart, W., and Nasmyth, K. (2011). Cohesin's concatenation of sister DNAs maintains their intertwining. Mol. Cell **44:** 97–107.

Fransz, P.F., Alonso-Blanco, C., Liharska, T.B., Peeters, A.J.M., Zabel, P., and de Jong, J.H. (1996). High-resolution physical mapping in *Arabidopsis thaliana* and tomato by fluorescence in situ hybridization to extended DNA fibers. Plant J. **9:** 421–430.

Gandhi, R., Gillespie, P.J., and Hirano, T. (2006). Human Wapl is a cohesin-binding protein that promotes sister-chromatid resolution in mitotic prophase. Curr. Biol. **16:** 2406–2417.

Gerlich, D., Koch, B., Dupeux, F., Peters, J.M., and Ellenberg, J. (2006). Live-cell imaging reveals a stable cohesin-chromatin interaction after but not before DNA replication. Curr. Biol. **16:** 1571–1578.

Giménez-Abián, J.F., Sumara, I., Hirota, T., Hauf, S., Gerlich, D., de la Torre, C., Ellenberg, J., and Peters, J.M. (2004). Regulation of sister chromatid cohesion between chromosome arms. Curr. Biol. **14:** 1187–1193.

Guacci, V., and Koshland, D. (2012). Cohesin-independent segregation of sister chromatids in budding yeast. Mol. Biol. Cell **23:** 729–739.

Haarhuis, J.H., Elbatsh, A.M., and Rowland, B.D. (2014). Cohesin and its regulation: on the logic of X-shaped chromosomes. Dev. Cell **31:** 7–18.

Haarhuis, J.H., Elbatsh, A.M., van den Broek, B., Camps, D., Erkan, H., Jalink, K., Medema, R.H., and Rowland, B.D. (2013). WAPL-mediated removal of cohesin protects against segregation errors and aneuploidy. Curr. Biol. **23:** 2071–2077.

Haering, C.H., Löwe, J., Hochwagen, A., and Nasmyth, K. (2002). Molecular architecture of SMC proteins and the yeast cohesin complex. Mol. Cell **9:** 773–788.

Hauf, S., Roitinger, E., Koch, B., Dittrich, C.M., Mechtler, K., and Peters, J.-M. (2005). Dissociation of cohesin from chromosome arms and loss of arm cohesion during early mitosis depends on phosphorylation of SA2. PLoS Biol. **3:** e69.

Hauf, S., Waizenegger, I.C., and Peters, J.M. (2001). Cohesin cleavage by separase required for anaphase and cytokinesis in human cells. Science **293:** 1320–1323.

Herr, J.M., Jr. (1971). A new clearing-squash technique for the study of ovule development in angiosperms. Am. J. Bot. **58:** 785–790.

Higgins, J.D., Sanchez-Moran, E., Armstrong, S.J., Jones, G.H., and Franklin, F.C.H. (2005). The Arabidopsis synaptonemal complex protein ZYP1 is required for chromosome synapsis and normal fidelity of crossing over. Genes Dev. **19:** 2488–2500.

Jiang, L., Yuan, L., Xia, M., and Makaroff, C.A. (2010). Proper levels of the Arabidopsis cohesion establishment factor CTF7 are essential for embryo and megagametophyte, but not endosperm, development. Plant Physiol. **154:** 820–832.

Kamath, R.S., et al. (2003). Systematic functional analysis of the *Caenorhabditis elegans* genome using RNAi. Nature **421:** 231–237.

Kanellopoulou, C., Muljo, S.A., Kung, A.L., Ganesan, S., Drapkin, R., Jenuwein, T., Livingston, D.M., and Rajewsky, K. (2005). Dicer-deficient mouse embryonic stem cells are defective in differentiation and centromeric silencing. Genes Dev. **19:** 489–501.

Kitajima, T.S., Hauf, S., Ohsugi, M., Yamamoto, T., and Watanabe, Y. (2005). Human Bub1 defines the persistent cohesion site along the mitotic chromosome by affecting Shugoshin localization. Curr. Biol. **15:** 353–359.

Kozak, J., West, C.E., White, C., da Costa-Nunes, J.A., and Angelis, K.J. (2009). Rapid repair of DNA double strand breaks in *Arabidopsis thaliana* is dependent on proteins involved in chromosome structure maintenance. DNA Repair (Amst.) **8:** 413–419.

Kueng, S., Hegemann, B., Peters, B.H., Lipp, J.J., Schleiffer, A., Mechtler, K., and Peters, J.M. (2006). Wapl controls the dynamic association of cohesin with chromatin. Cell **127:** 955–967.

Lafont, A.L., Song, J., and Rankin, S. (2010). Sororin cooperates with the acetyltransferase Eco2 to ensure DNA replication-dependent sister chromatid cohesion. Proc. Natl. Acad. Sci. USA **107:** 20364–20369.

Lam, W.S., Yang, X., and Makaroff, C.A. (2005). Characterization of *Arabidopsis thaliana* SMC1 and SMC3: evidence that AtSMC3 may function beyond chromosome cohesion. J. Cell Sci. **118:** 3037–3048.

Lénárt, P., Petronczki, M., Steegmaier, M., Di Fiore, B., Lipp, J.J., Hoffmann, M., Rettig, W.J., Kraut, N., and Peters, J.-M. (2007). The small-molecule inhibitor BI 2536 reveals novel insights into mitotic roles of polo-like kinase 1. Curr. Biol. **17:** 304–315.

Liu, D., and Makaroff, C.A. (2015). Overexpression of a truncated CTF7 construct leads to pleiotropic defects in reproduction and vegetative growth in Arabidopsis. BMC Plant Biol. **15:** 74.

Liu, Z., and Makaroff, C.A. (2006). Arabidopsis separase AESP is essential for embryo development and the release of cohesin during meiosis. Plant Cell **18:** 1213–1225.

Lopez-Serra, L., Lengronne, A., Borges, V., Kelly, G., and Uhlmann, F. (2013). Budding yeast Wapl controls sister chromatid cohesion maintenance and chromosome condensation. Curr. Biol. **23:** 64–69.

Losada, A., Hirano, M., and Hirano, T. (2002). Cohesin release is required for sister chromatid resolution, but not for condensin-mediated compaction, at the onset of mitosis. Genes Dev. **16:** 3004–3016.

Lu, S., Goering, M., Gard, S., Xiong, B., McNairn, A.J., Jaspersen, S.L., and Gerton, J.L. (2010). Eco1 is important for DNA damage repair in *S. cerevisiae.* Cell Cycle **9:** 3315–3327.

Luo, D., Bernard, D.G., Balk, J., Hai, H., and Cui, X. (2012). The DUF59 family gene AE7 acts in the cytosolic iron-sulfur cluster assembly pathway to maintain nuclear genome integrity in Arabidopsis. Plant Cell **24:** 4135–4148.

Martinez-Zapater, J., Estelle, M., and Somerville, C. (1986). A highly repeated DNA sequence in *Arabidopsis thaliana.* Mol. Gen. Genet. **204:** 417–423.

McGuinness, B.E., Hirota, T., Kudo, N.R., Peters, J.M., and Nasmyth, K. (2005). Shugoshin prevents dissociation of cohesin from centromeres during mitosis in vertebrate cells. PLoS Biol. **3:** e86.

Moissiard, G., et al. (2012). MORC family ATPases required for heterochromatin condensation and gene silencing. Science **336:** 1448–1451.

Musacchio, A., and Salmon, E.D. (2007). The spindle-assembly checkpoint in space and time. Nat. Rev. Mol. Cell Biol. **8:** 379–393.

Nasmyth, K. (2011). Cohesin: a catenase with separate entry and exit gates? Nat. Cell Biol. **13:** 1170–1177.

Nasmyth, K., and Haering, C.H. (2009). Cohesin: its roles and mechanisms. Annu. Rev. Genet. **43:** 525–558.

Nezames, C.D., Sjogren, C.A., Barajas, J.F., and Larsen, P.B. (2012). The Arabidopsis cell cycle checkpoint regulators TANMEI/ALT2 and ATR mediate the active process of aluminum-dependent root growth inhibition. Plant Cell **24:** 608–621.

Nishiyama, T., Ladurner, R., Schmitz, J., Kreidl, E., Schleiffer, A., Bhaskara, V., Bando, M., Shirahige, K., Hyman, A.A., Mechtler, K., and Peters, J.M. (2010). Sororin mediates sister chromatid cohesion by antagonizing Wapl. Cell **143:** 737–749.

Ouyang, Z., Zheng, G., Song, J., Borek, D.M., Otwinowski, Z., Brautigam, C.A., Tomchick, D.R., Rankin, S., and Yu, H. (2013). Structure of the human cohesin inhibitor Wapl. Proc. Natl. Acad. Sci. USA **110:** 11355–11360.

Peric-Hupkes, D., and van Steensel, B. (2008). Linking cohesin to gene regulation. Cell **132:** 925–928.

Peters, J.M., Tedeschi, A., and Schmitz, J. (2008). The cohesin complex and its roles in chromosome biology. Genes Dev. **22:** 3089–3114.

Pradillo, M., Knoll, A., Oliver, C., Varas, J., Corredor, E., Puchta, H., and Santos, J.L. (2015). Involvement of the cohesin cofactor PDS5 (SPO76) during meiosis and DNA repair in *Arabidopsis thaliana.* Front. Plant Sci. **6:** 1034.

Rolef Ben-Shahar, T., Heeger, S., Lehane, C., East, P., Flynn, H., Skehel, M., and Uhlmann, F. (2008). Eco1-dependent cohesin acetylation during establishment of sister chromatid cohesion. Science **321:** 563–566.

Ross, K.J., Fransz, P., and Jones, G.H. (1996). A light microscopic atlas of meiosis in *Arabidopsis thaliana*. Chromosome Res. **4:** 507–516.

Rowland, B.D., et al. (2009). Building sister chromatid cohesion: smc3 acetylation counteracts an antiestablishment activity. Mol. Cell **33:** 763–774.

Salic, A., Waters, J.C., and Mitchison, T.J. (2004). Vertebrate shugoshin links sister centromere cohesion and kinetochore microtubule stability in mitosis. Cell **118:** 567–578.

Schmitz, J., Watrin, E., Lénárt, P., Mechtler, K., and Peters, J.M. (2007). Sororin is required for stable binding of cohesin to chromatin and for sister chromatid cohesion in interphase. Curr. Biol. **17:** 630–636.

Schvartzman, J.M., Sotillo, R., and Benezra, R. (2010). Mitotic chromosomal instability and cancer: mouse modelling of the human disease. Nat. Rev. Cancer **10:** 102–115.

Seitan, V.C., and Merkenschlager, M. (2012). Cohesin and chromatin organisation. Curr. Opin. Genet. Dev. **22:** 93–100.

Shintomi, K., and Hirano, T. (2009). Releasing cohesin from chromosome arms in early mitosis: opposing actions of Wapl-Pds5 and Sgo1. Genes Dev. **23:** 2224–2236.

Siddiqi, I., Ganesh, G., Grossniklaus, U., and Subbiah, V. (2000). The dyad gene is required for progression through female meiosis in Arabidopsis. Development **127:** 197–207.

Singh, D.K., Andreuzza, S., Panoli, A.P., and Siddiqi, I. (2013). AtCTF7 is required for establishment of sister chromatid cohesion and association of cohesin with chromatin during meiosis in Arabidopsis. BMC Plant Biol. **13:** 117.

Siomos, M.F., Badrinath, A., Pasierbek, P., Livingstone, D., White, J., Glotzer, M., and Nasmyth, K. (2001). Separase is required for chromosome segregation during meiosis I in *Caenorhabditis elegans.* Curr. Biol. **11:** 1825–1835.

Skibbens, R.V., Corson, L.B., Koshland, D., and Hieter, P. (1999). Ctf7p is essential for sister chromatid cohesion and links mitotic chromosome structure to the DNA replication machinery. Genes Dev. **13:** 307–319.

Soppe, W.J., Jasencakova, Z., Houben, A., Kakutani, T., Meister, A., Huang, M.S., Jacobsen, S.E., Schubert, I., and Fransz, P.F. (2002). DNA methylation controls histone H3 lysine 9 methylation and heterochromatin assembly in Arabidopsis. EMBO J. **21:** 6549–6559.

Sumara, I., Vorlaufer, E., Stukenberg, P.T., Kelm, O., Redemann, N., Nigg, E.A., and Peters, J.M. (2002). The dissociation of cohesin from chromosomes in prophase is regulated by Polo-like kinase. Mol. Cell **9:** 515–525.

Sutani, T., Kawaguchi, T., Kanno, R., Itoh, T., and Shirahige, K. (2009). Budding yeast Wpl1(Rad61)-Pds5 complex counteracts sister chromatid cohesion-establishing reaction. Curr. Biol. **19:** 492–497.

Tang, Z., Shu, H., Qi, W., Mahmood, N.A., Mumby, M.C., and Yu, H. (2006). PP2A is required for centromeric localization of Sgo1 and proper chromosome segregation. Dev. Cell **10:** 575–585.

Tedeschi, A., et al. (2013). Wapl is an essential regulator of chromatin structure and chromosome segregation. Nature **501:** 564–568.

Tong, K., and Skibbens, R.V. (2015). Pds5 regulators segregate cohesion and condensation pathways in *Saccharomyces cerevisiae.* Proc. Natl. Acad. Sci. USA **112:** 7021–7026.

Tóth, A., Ciosk, R., Uhlmann, F., Galova, M., Schleiffer, A., and Nasmyth, K. (1999). Yeast cohesin complex requires a conserved protein, Eco1p(Ctf7), to establish cohesion between sister chromatids during DNA replication. Genes Dev. **13:** 320–333.

Uhlmann, F., Lottspeich, F., and Nasmyth, K. (1999). Sister-chromatid separation at anaphase onset is promoted by cleavage of the cohesin subunit Scc1. Nature **400:** 37–42.

Unal, E., Heidinger-Pauli, J.M., Kim, W., Guacci, V., Onn, I., Gygi, S.P., and Koshland, D.E. (2008). A molecular determinant for the establishment of sister chromatid cohesion. Science **321:** 566–569.

van der Lelij, P., et al. (2009). The cellular phenotype of Roberts syndrome fibroblasts as revealed by ectopic expression of ESCO2. PLoS One **4:** e6936.

van der Waal, M.S., Hengeveld, R.C.C., van der Horst, A., and Lens, S.M.A. (2012). Cell division control by the Chromosomal Passenger Complex. Exp. Cell Res. **318:** 1407–1420.

Vega, H., et al. (2005). Roberts syndrome is caused by mutations in ESCO2, a human homolog of yeast ECO1 that is essential for the establishment of sister chromatid cohesion. Nat. Genet. **37:** 468–470.

Vernì, F., Gandhi, R., Goldberg, M.L., and Gatti, M. (2000). Genetic and molecular analysis of wings apart-like (wapl), a gene controlling heterochromatin organization in *Drosophila melanogaster*. Genetics **154:** 1693–1710.

Vielle-Calzada, J.P., Baskar, R., and Grossniklaus, U. (2000). Delayed activation of the paternal genome during seed development. Nature **404:** 91–94.

Wang, L.H.-C., Mayer, B., Stemmann, O., and Nigg, E.A. (2010). Centromere DNA decatenation depends on cohesin removal and is required for mammalian cell division. J. Cell Sci. **123:** 806–813.

Watanabe, Y. (2005). Shugoshin: guardian spirit at the centromere. Curr. Opin. Cell Biol. **17:** 590–595.

Whelan, G., Kreidl, E., Wutz, G., Egner, A., Peters, J.M., and Eichele, G. (2012). Cohesin acetyltransferase Esco2 is a cell viability factor and is required for cohesion in pericentric heterochromatin. EMBO J. **31:** 71–82.

Yamagishi, Y., Sakuno, T., Shimura, M., and Watanabe, Y. (2008). Heterochromatin links to centromeric protection by recruiting shugoshin. Nature **455:** 251–255.

Yang, X., Boateng, K.A., Strittmatter, L., Burgess, R., and Makaroff, C.A. (2009). Arabidopsis separase functions beyond the removal of sister chromatid cohesion during meiosis. Plant Physiol. **151:** 323–333.

Yuan, L., Yang, X., Ellis, J.L., Fisher, N.M., and Makaroff, C.A. (2012). The Arabidopsis SYN3 cohesin protein is important for early meiotic events. Plant J. **71:** 147–160.

Yuan, L., Yang, X., and Makaroff, C.A. (2011). Plant cohesins, common themes and unique roles. Curr. Protein Pept. Sci. **12:** 93–104.

Zhang, J., et al. (2008). Acetylation of Smc3 by Eco1 is required for S phase sister chromatid cohesion in both human and yeast. Mol. Cell **31:** 143–151.